AD-A155 225 CIRCULATION ANALYSIS OF TWO SNOWSTORMS DURING THE SNOW-TWO PROGRAM(U) OPHIR CORP LAKEWOOD CO Y L CHEN SEP 84 SCIENTIFIC-1 AFGL-TR-84-0255 F19628-83-C-0130 1/1

UNCLASSIFIED F/G 4/2 NL

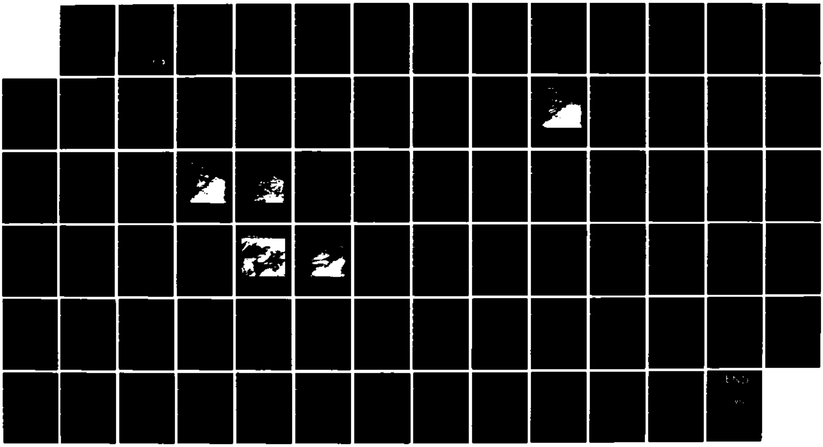

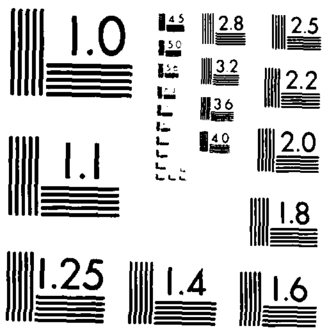

MICROCOPY RESOLUTION TEST CHART
NATIONAL BUREAU OF STANDARDS 1963-A

AD-A155 225

AFGL-TR-84-0255

CIRCULATION ANALYSIS OF TWO SNOWSTORMS DURING THE SNOW-TWO PROGRAM

Dr. Yi-Leng Chen

OPHIR Corporation
7333 West Jefferson Avenue, Suite 210
Lakewood, CO 80235

SCIENTIFIC REPORT NO. 1

September 1984

Approved for public release; distribution unlimited

AIR FORCE GEOPHYSICS LABORATORY
AIR FORCE SYSTEMS COMMAND
UNITED STATES AIR FORCE
HANSCOM AFB, MASSACHUSETTS 01731

85 5 17

"This technical report has been reviewed and is approved for publication"

Barbara A. Main

BARBARA A. MAIN
Contract Manager

Arnold A. Barnes, Jr.

ARNOLD A. BARNES, JR., Chief
Cloud Physics Branch

FOR THE COMMANDER

Robert A. McClatchey

ROBERT A. McCLATCHEY, Director
Atmospheric Sciences Division

This report has been reviewed by the ESD Public Affairs Office (PA) and is releasable to the National Technical Information Service (NTIS).

Qualified requestors may obtain additional copies from the Defense Technical Information Center. All others should apply to the National Technical Information Service.

If your address has changed, or if you wish to be removed from the mailing list, or if the addressee is no longer employed by your organization, please notify AFGL/DAA/LYC, Hanscom AFB, MA 01731. This will assist us in maintaining a current mailing list.

Unclassified

SECURITY CLASSIFICATION OF THIS PAGE

REPORT DOCUMENTATION PAGE

1a. REPORT SECURITY CLASSIFICATION
Unclassified

1b. RESTRICTIVE MARKINGS

2a. SECURITY CLASSIFICATION AUTHORITY

2b. DECLASSIFICATION/DOWNGRADING SCHEDULE

3. DISTRIBUTION/AVAILABILITY OF REPORT
Approved for public release;
distribution unlimited

4. PERFORMING ORGANIZATION REPORT NUMBER(S)

5. MONITORING ORGANIZATION REPORT NUMBER(S)
AFGL-TR-84-0255

6a. NAME OF PERFORMING ORGANIZATION
Ophir Corp
7333 West Jefferson Ave

6b. OFFICE SYMBOL *(If applicable)*

7a. NAME OF MONITORING ORGANIZATION
Air Force Geophysics Laboratory

6c. ADDRESS *(City, State and ZIP Code)*
Suite 210
Lakewood, Colorado 80235

7b. ADDRESS *(City, State and ZIP Code)*
Hanscom AFB, Massachusetts 01731
Monitor/Barbara A. Main/LYC

8a. NAME OF FUNDING/SPONSORING ORGANIZATION

8b. OFFICE SYMBOL *(If applicable)*

9. PROCUREMENT INSTRUMENT IDENTIFICATION NUMBER
F19628-83-C-0130

8c. ADDRESS *(City, State and ZIP Code)*

10. SOURCE OF FUNDING NOS.

PROGRAM ELEMENT NO.	PROJECT NO.	TASK NO.	WORK UNIT NO.
62101F	6670	12	CA

11. TITLE *(Include Security Classification)*
See reverse side

12. PERSONAL AUTHOR(S)
Yi-Leng Chen

13a. TYPE OF REPORT
Sci Rpt No. 1

13b. TIME COVERED
FROM 1/16/84 TO 8/31/84

14. DATE OF REPORT *(Yr., Mo., Day)*
1984 September

15. PAGE COUNT
68

16. SUPPLEMENTARY NOTATION

17. COSATI CODES

FIELD	GROUP	SUB. GR.
04	02	

18. SUBJECT TERMS *(Continue on reverse if necessary and identify by block number)*
Meteorology, Snowstorms;
Dynamics, Cloud formation.

19. ABSTRACT *(Continue on reverse if necessary and identify by block number)*

In this study, the conditions during two snowstorm cases during SNOW TWO, 16-17 January and 23-24 January, 1984, were analyzed. In an effort to incorporate large-scale forcing, the kinematic method (so as to include the effects of latent heat release and convective transport) was used to compute the large-scale vertical motion. This large-scale vertical motion computed, as well as other conditions studied for both cases, will provide useful information for the proper choice of initial conditions for future numerical simulations of cloud development.

20. DISTRIBUTION/AVAILABILITY OF ABSTRACT
UNCLASSIFIED/UNLIMITED ☒ SAME AS RPT ☐ DTIC USERS ☐

21. ABSTRACT SECURITY CLASSIFICATION
Unclassified

22a. NAME OF RESPONSIBLE INDIVIDUAL
Barbara A. Main

22b. TELEPHONE NUMBER *(Include Area Code)*
(617)861-2947

22c. OFFICE SYMBOL
LYC

DD FORM 1473, 83 APR EDITION OF 1 JAN 73 IS OBSOLETE.

Unclassified

SECURITY CLASSIFICATION OF THIS PAGE

Block 11

CIRCULATION ANALYSIS OF TWO SNOWSTORMS DURING THE SNOW-TWO PROGRAM

CONTENTS

LIST OF FIGURES

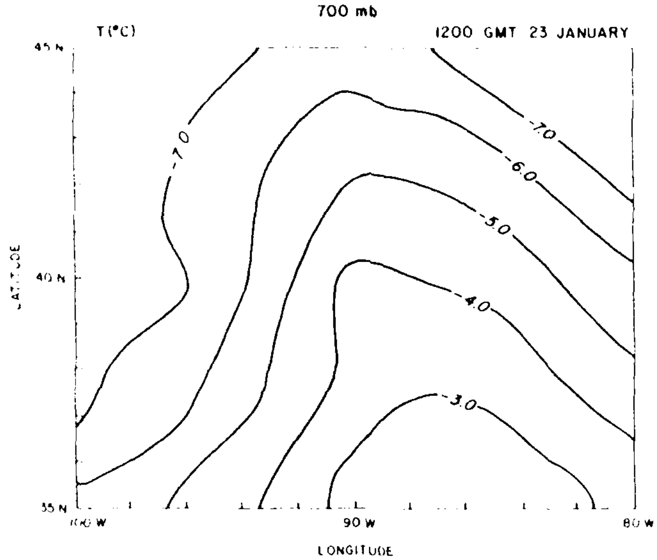

Figure 12. Horizontal Distributions of Temperature at the 700 mb Level for 1200 GMT on 23 January 1984.

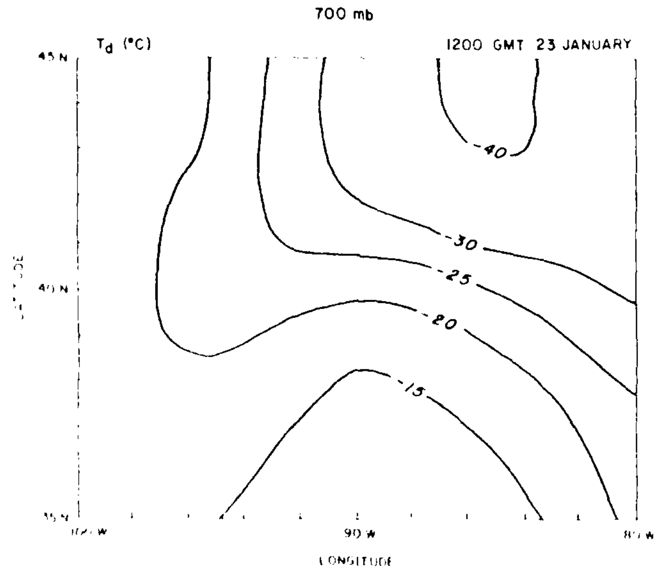

Figure [illegible]. Horizontal Distributions of Dew Point Temperature at the 700 mb Level for 1200 GMT on 23 January 1984.

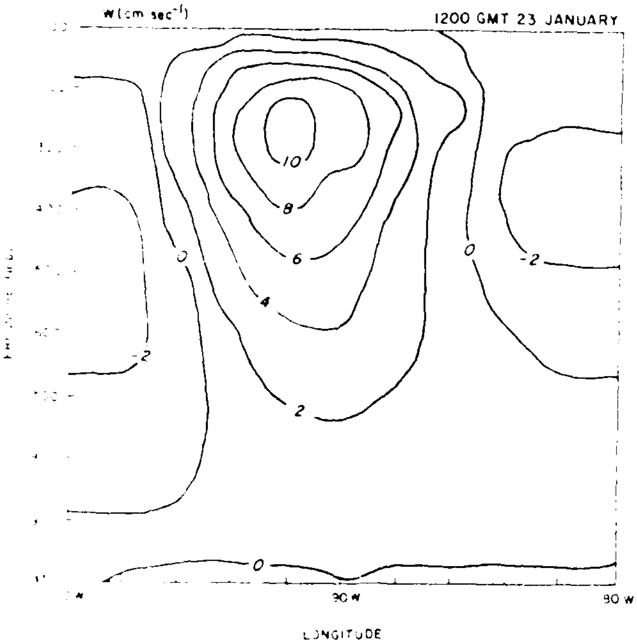

Figure 11. Vertical, West-East Cross Sections of Vertical Velocity averaged from 40 degrees N through 42 degrees N for 1200 GMT on 23 January 1984.

The convergence associated with the outflow layer in the upper troposphere at 80 degrees W was found above 300 mb (Figure 10). A deep layer of convergence was evident below 300 mb between 85 and 95 degrees W with relatively strong convergence near the surface and in the mid-troposphere in the area of deep convection.

The change of the thermodynamic structure due to the development of southerly flow, horizontal distributions of temperature, dew point temperature, and meridional wind at 700 mb is shown in Figures 12 through 15. A warm and moist tongue was found near 90 degrees W (Figures 12 & 13) together with a strong meridional (southerly) wind with speeds as high as 15 m sec^{-1} (Figure 14). The horizontal distribution of vertical motion at 700 mb (Figure 15) shows the upward motion was present near 90 degrees W as well. It is apparent that the strong southerly flow advected the warm and moist air to the area of convection in low levels and changed the atmospheric stability. The large-scale lifting provided the lifting required for the release of potential instability. The divergence associated with the outflow layer computed above 300 mb (Figure 10) indicated deep convective clouds developed for this case in agreement with the cold cloud top temperature observed by the GOES-East infrared pictures.

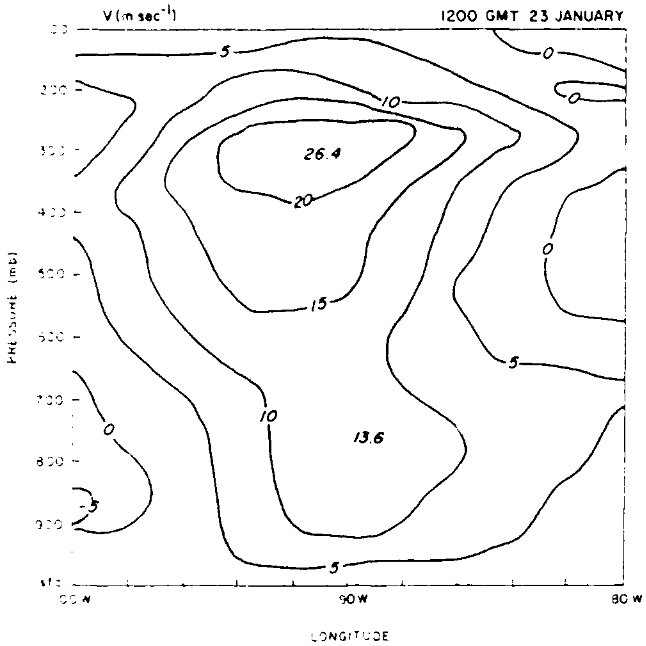

Figure 9. Vertical, West-East Cross Sections of Meridional Wind Averaged from 40 degrees N through 42 degrees N for 1200 GMT on 23 January 1984.

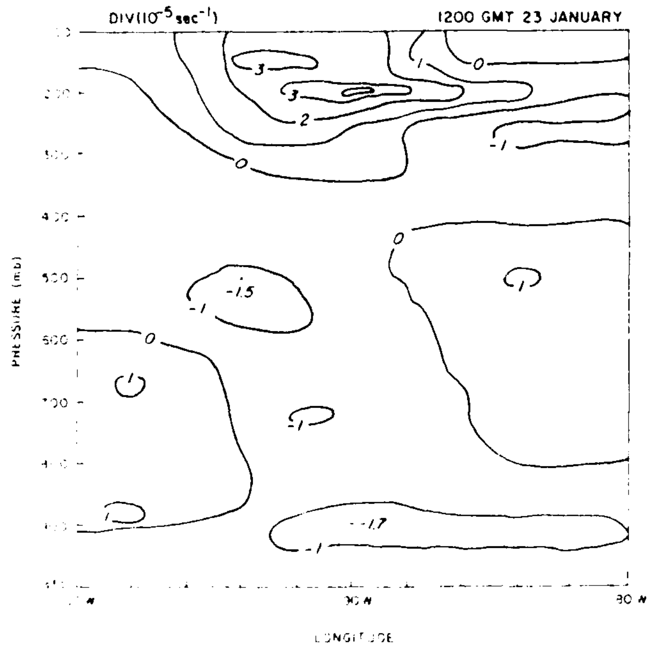

Figure 10. Vertical, West-East Cross Sections of Divergence Averaged from 40 degrees N through 42 degrees N for 1200 GMT on 23 January 1984.

At 1200 GMT 23 January, strong low-level warm advection was evident in the area near 90 degrees W from the surface (Figure 3), 850 mb (Figure 4), and 700 mb (Figure 5), constant pressure charts. The axis of with coldest cloud top temperature from the GOES-East infrared picture at 1200 GMT 23 January (Figure 7) was found 10 degrees to 15 degrees east of the surface trough. This is the region with strong low-level warm advection. A cut-off low associated with the surface trough in the upper troposphere was formed (Figure 6). Eventually this trough developed into a cold front at the East coast at 0000 GMT 25 January.

3.2 Results of the Analyses

The west-east cross sections averaged between 40 degrees to 42 degrees N for the zonal (westerly) wind (Figure 8), meridional (southerly) wind (Figure 9), divergence (Figure 10), and vertical motion for 1200 GMT 23 January (Figure 11). The most striking feature is that the region of upward motion coincided with the axis of maximum meridional wind around 90 degrees W (Figures 9 & 11). As noted before, this is the area where the convective activity is most intense (Figure 7). Subsidence was found both ahead of and behind the axis of maximum meridional wind where the convection was suppressed (Figure 11).

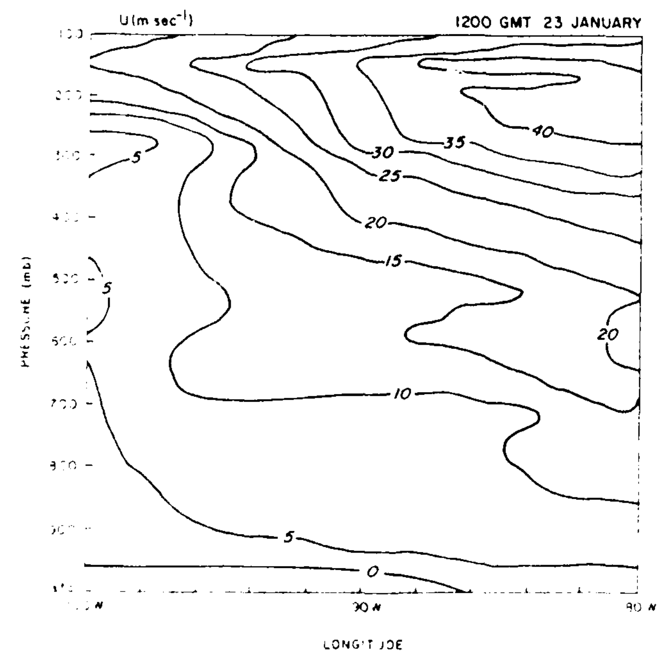

Figure 8. Vertical, West-East Cross Sections of Zonal Wind Averaged from 40 degrees N through 42 degrees N for 1200 GMT on 23 January 1984.

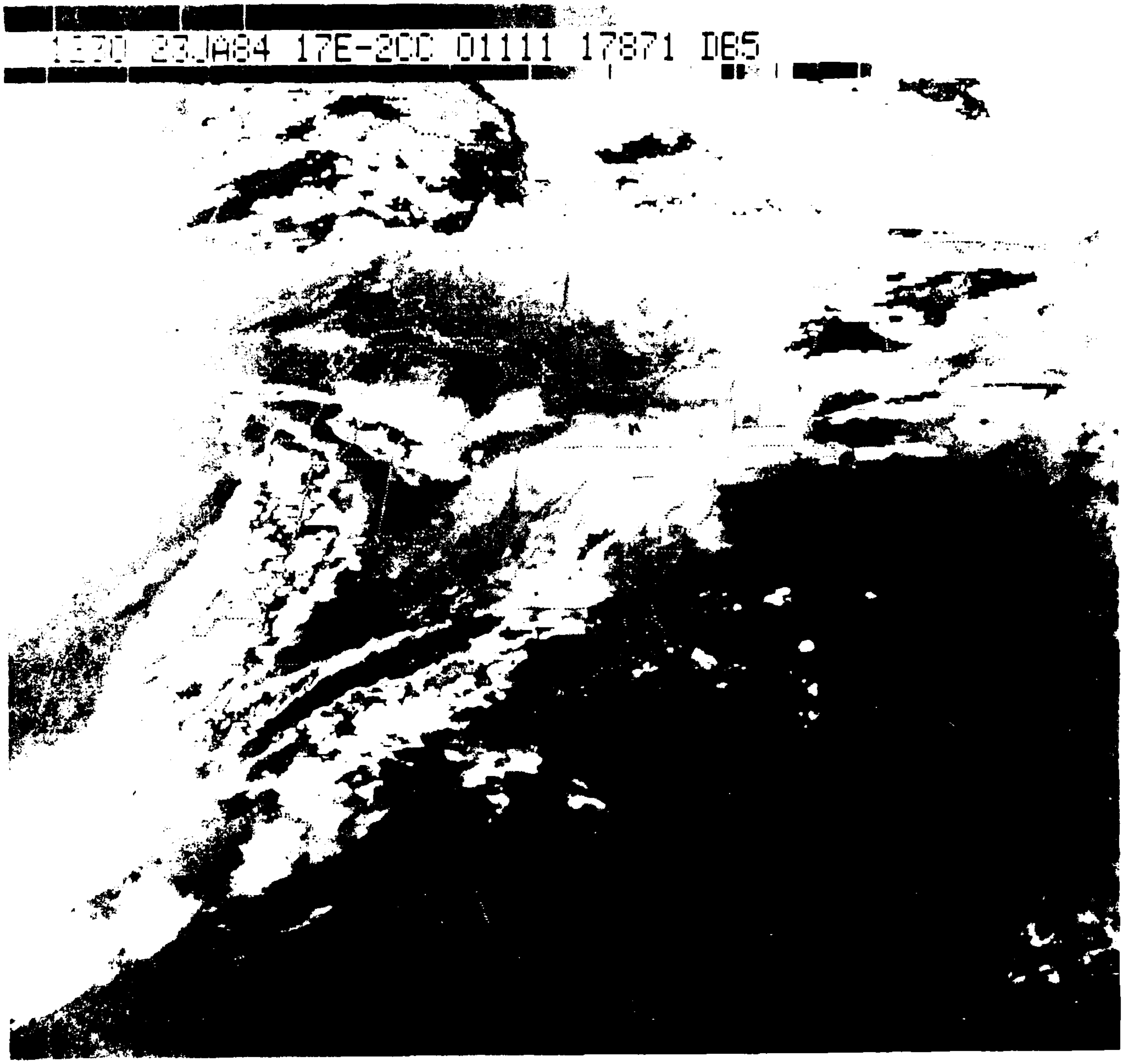

Figure 7. GOES-East Infrared Picture of the Eastern United States at 1230 GMT on 23 January 1984.

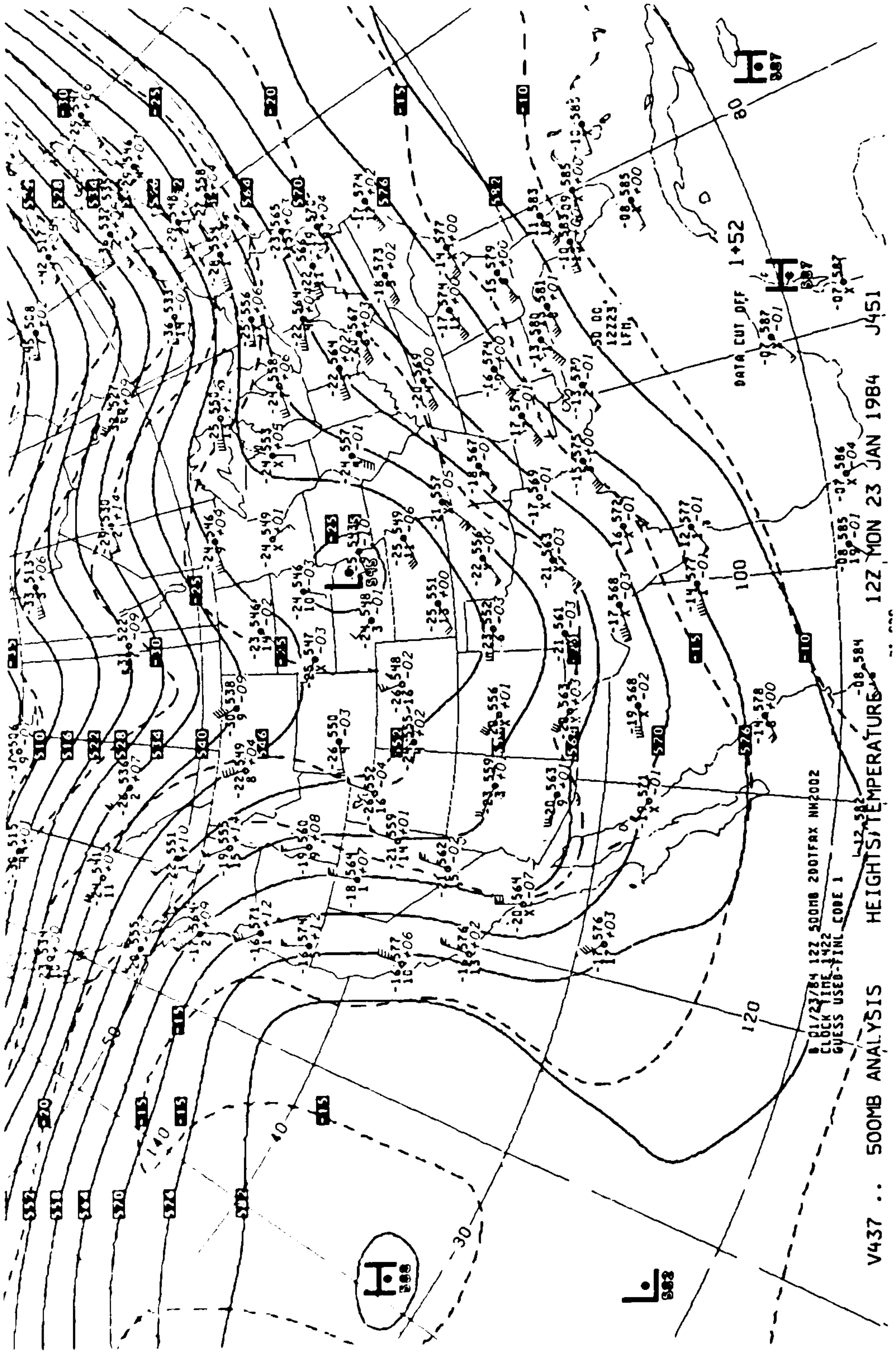

Figure 6. 500 mb Chart for 1200 GMT on 23 January 1984.

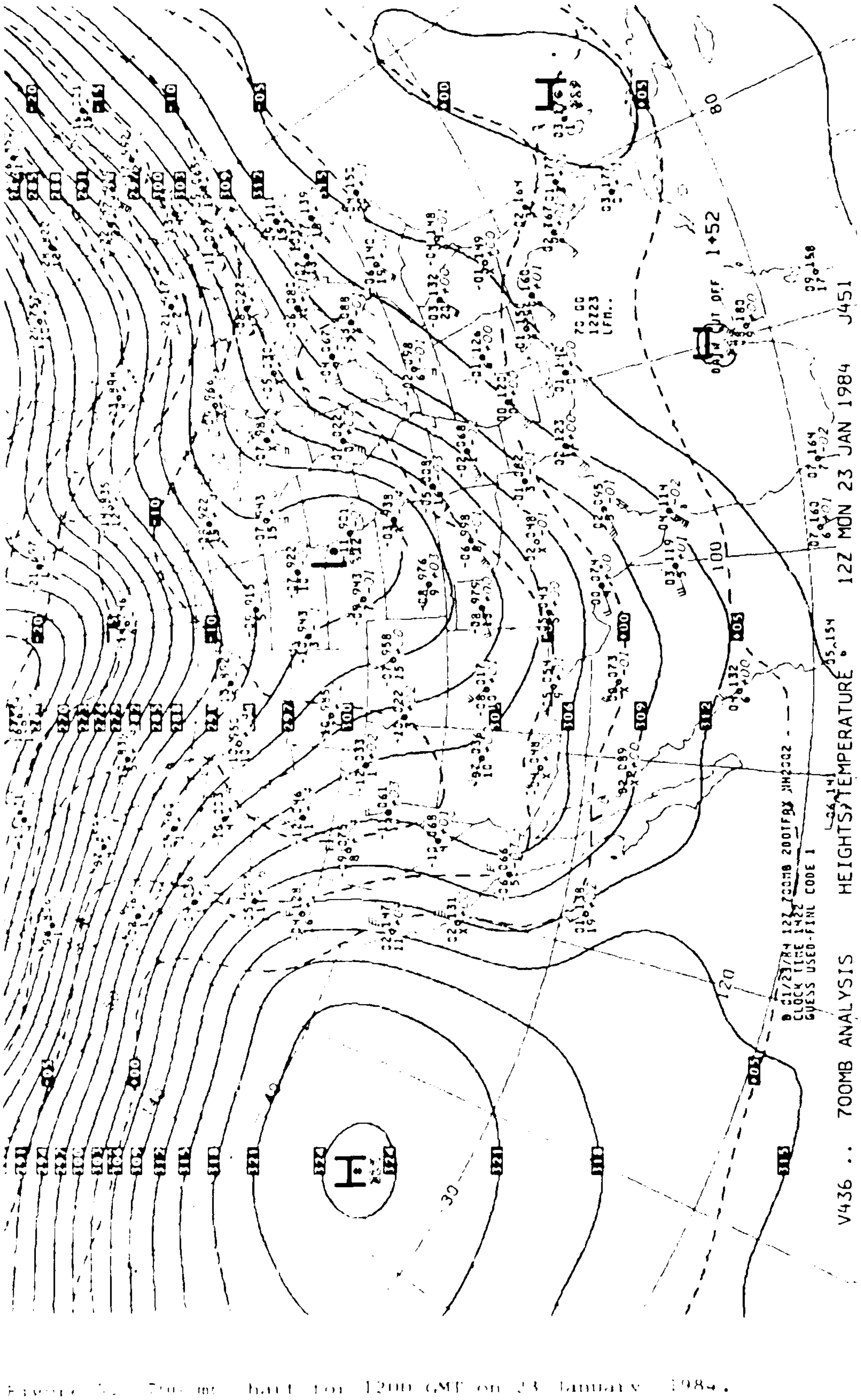

Figure 5. 700 mb chart for 1200 GMT on 23 January 1984.

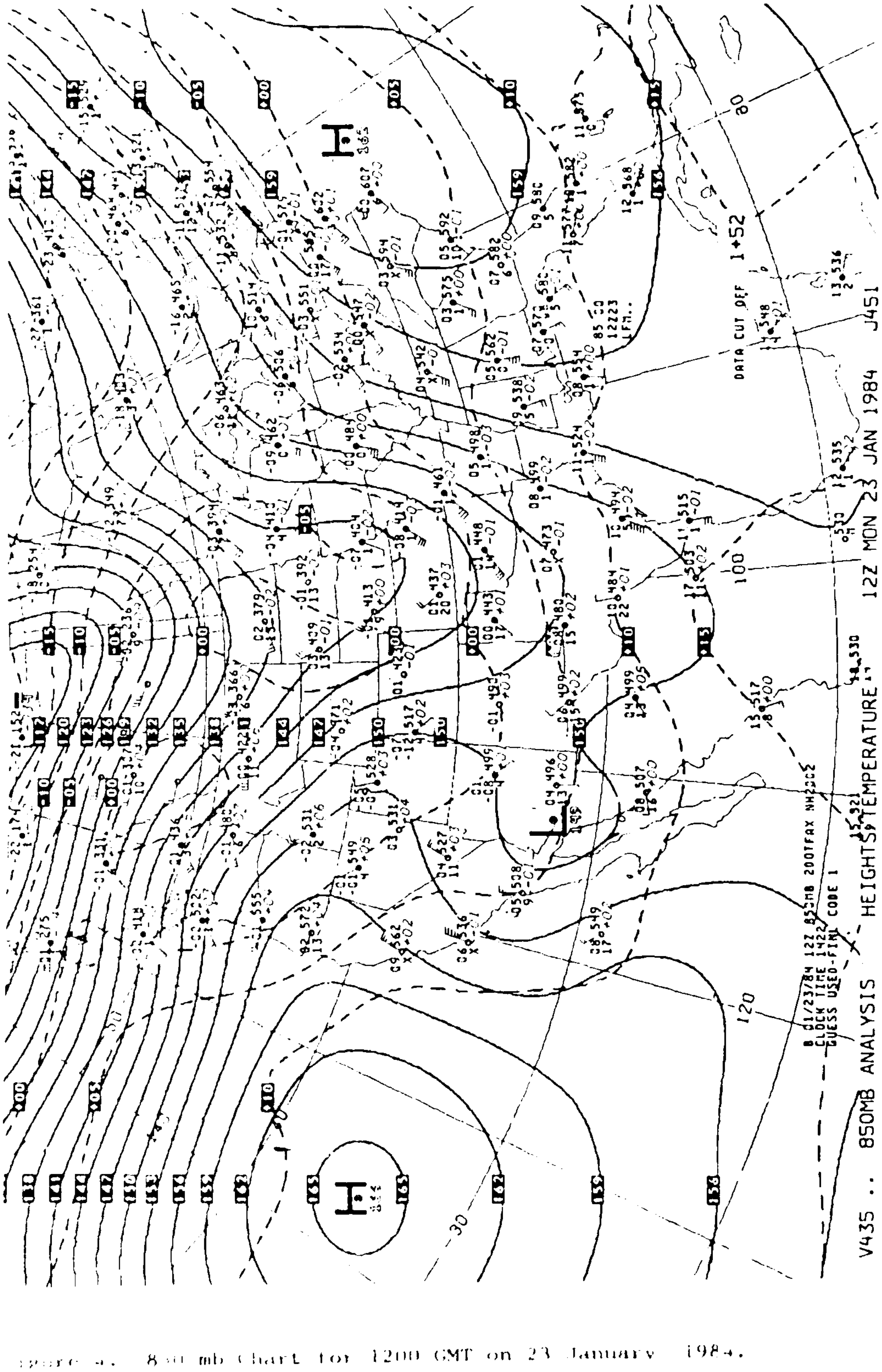

Figure 4. 850 mb Chart for 1200 GMT on 23 January 1984.

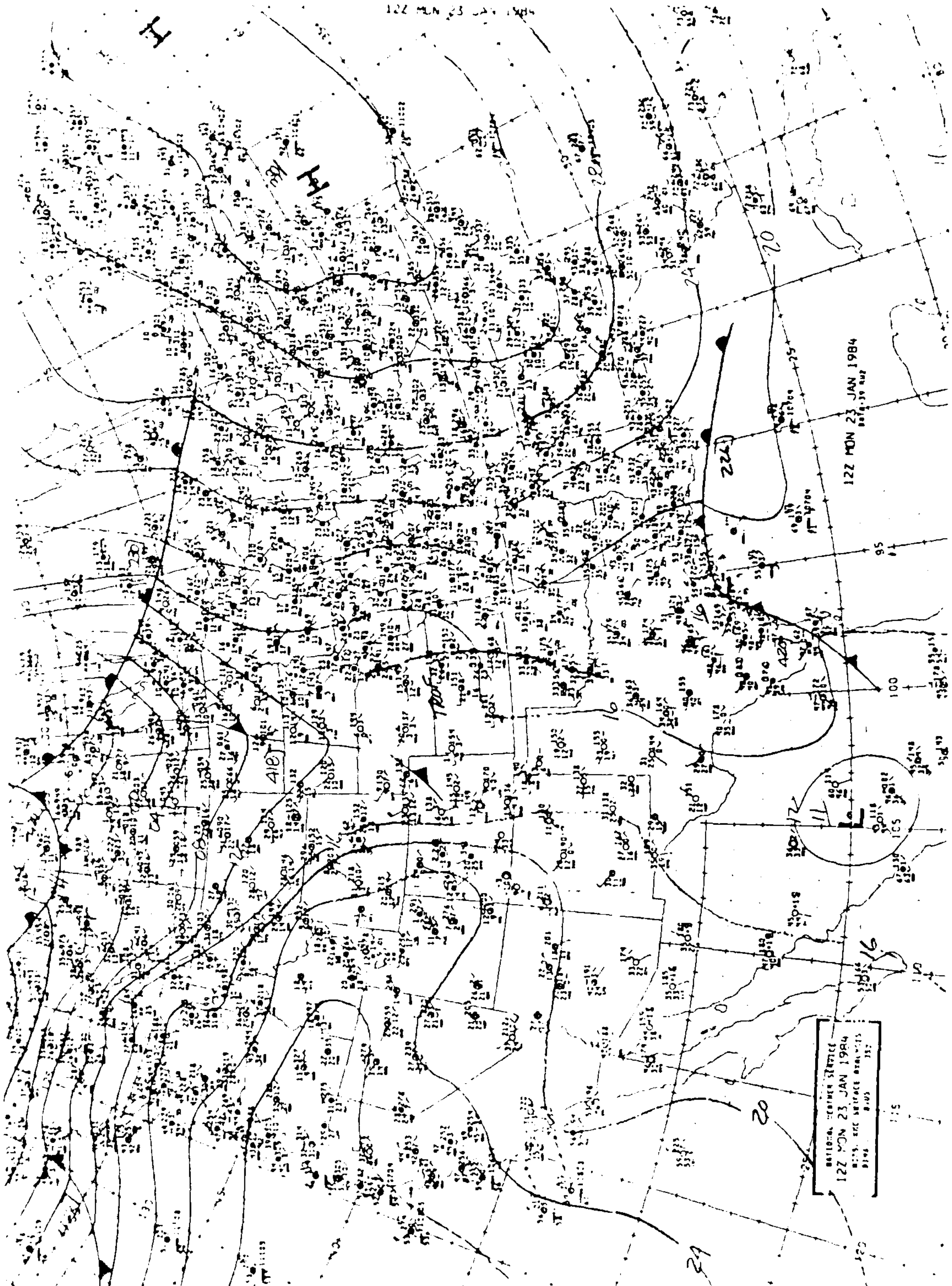

Figure 3. Surface Chart for 1200 GMT on 23 January 1984.

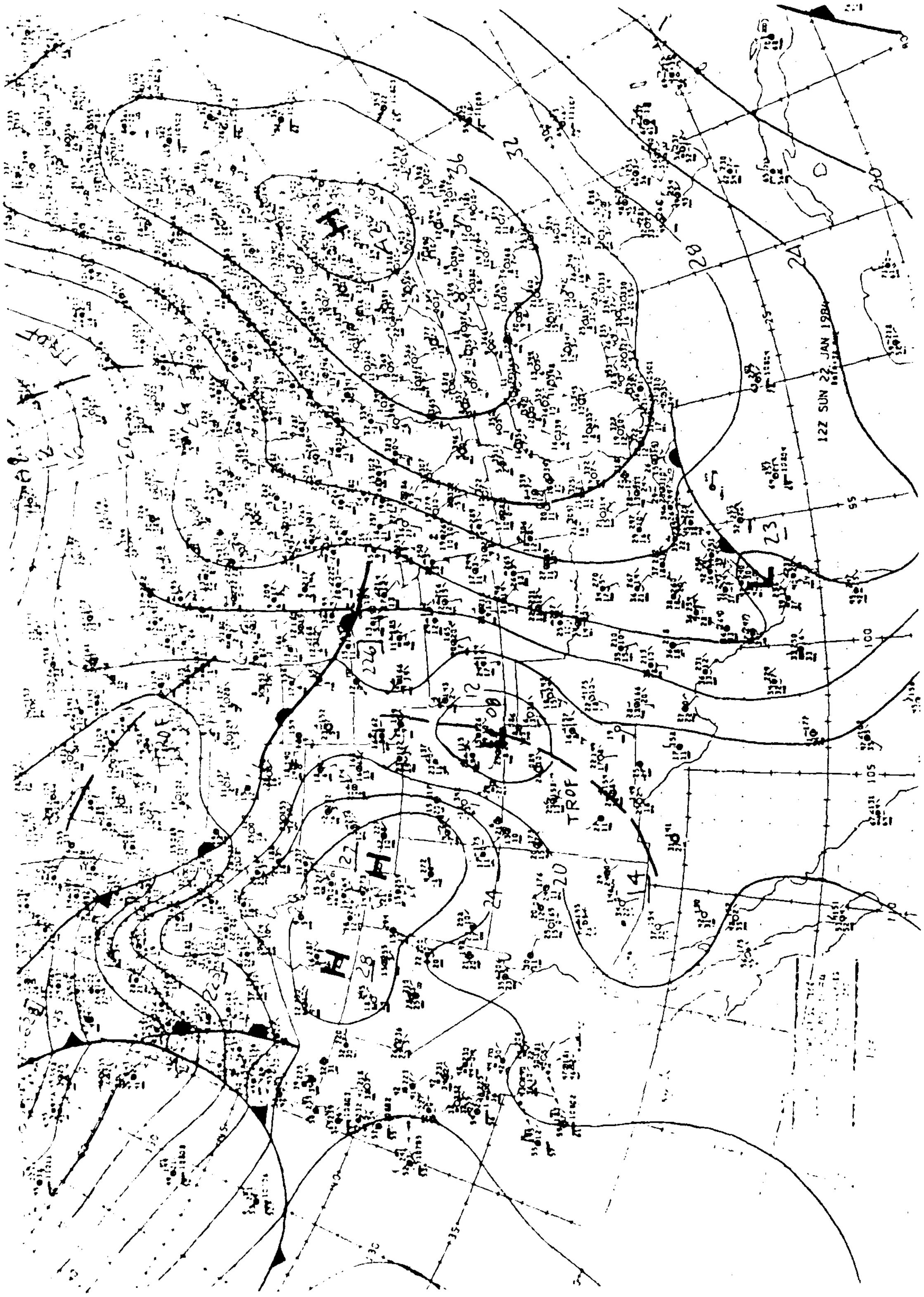

Figure 2. Surface Chart for 1200 GMT on 22 January 1984.

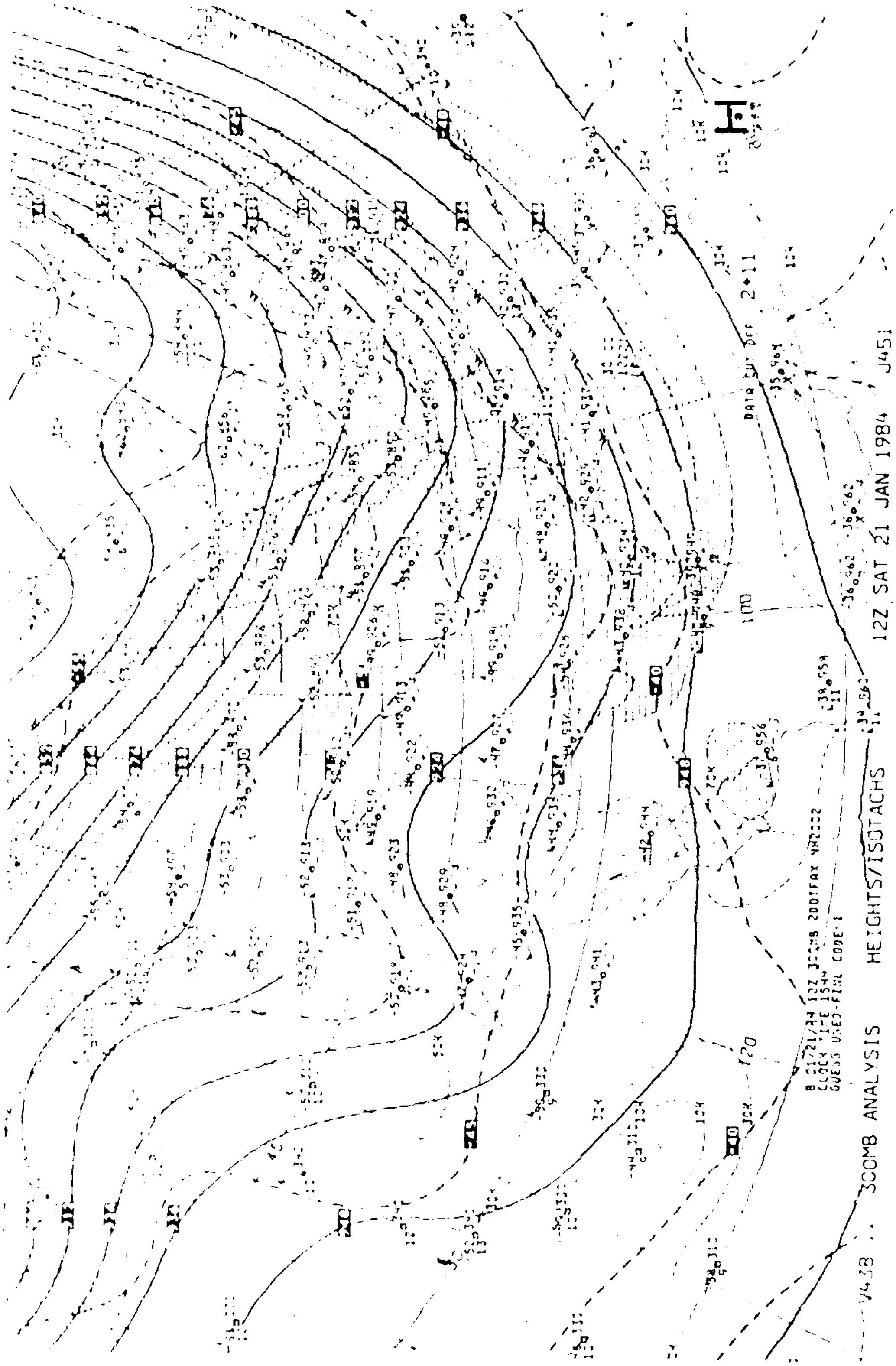

[illegible] Pressure Chart for 1200 GMT on 21 January [illegible]

The vertical p-velocity was calculated kinematically. The [w] field at the topographic level was calculated by:

$$\omega_G = -\rho g W_G = \rho g \vec{V}_G \cdot \vec{\nabla} H \qquad (1)$$

where ρ is the air density, [g] the gravitational acceleration, V_G the wind at the ground surface, and [H] the height of the surface. The horizontal divergence was estimated by:

$$\nabla \cdot \vec{v} = \frac{\delta u}{\delta x} + \frac{\delta v}{\delta y} - \frac{v}{R} \tan(\phi) \qquad (2)$$

where [R] is the radius of the earth and ϕ is the latitude. The term $(-\frac{v}{R}\tan\phi)$ is retained due to convergences of the meridians. The original estimates of divergence and [w] were corrected to ensure that [w] vanishes at 100 mb. The correction was made following O'Brien's (1970) scheme which assumes the errors in the divergent wind increases vertically as a linear function of pressure. Since the tropopause is approximately at 250 mb rather than 100 mb during the winter, a comparison between the vertical velocities obtained by imposing the upper boundary condition of [w] equal to zero at 100 mb and 200 mb was made in Appendix 1.

Finally, the vertical p-velocity was converted to cm sec^{-1} using the hydrostatic relationship.

The same objective analysis technique described above was applied to hourly surface observations. Details of the procedures to process upper-air data and surface observations are given in Appendix 2 and Appendix 3, respectively.

3. CASE OF 23-24 JANUARY

3.1 Synoptic Situation

At 1200 GMT 21 January 1984, the 300 mb constant pressure chart shows that an upper level trough was developing along the west coast (Figure 1). This trough was evident at the next observation time 0000 GMT 22 January for all constant pressure charts above 700 mb (not shown). As this trough intensified and propagated eastward, a surface trough was formed at 1200 GMT 22 January (Figure 2) in the southwest extending from Colorado to New Mexico. At the east coast a high pressure center was evident over Maryland and Virginia together with very cold temperatures in the eastern part of the United States. As the trough intensified, the west-east pressure gradient increased because of the high pressure center at the east coast and the developing trough in the west. The southerly flow ahead of the trough and behind the high pressure center strengthened and brought in the warm, moist air from the Gulf of Mexico replacing the cold, dry air in low levels.

Washington, D.C. were used to study the synoptic situation during snowstorm occurrences. The Defense Meteorological Satellite Program (DMSP) satellite photographs from the National Climate Center, Satellite Service Division D56, Washington D.C. and the Geostationary Operational Environmental Satellite (GOES)-East visible and infrared images, available from the McIDAS system at Air Force Geophysical Laboratory (AFGL), were also used.

Regular upper-air data in 12 hour intervals from National Weather Service rawinsonde station and hourly surface observations from stations within the domain of 75 degrees W to 105 degrees W and 25 degrees N to 60 degrees N were considered. The measurements for each sounding were not taken simultaneously. Furthermore, it takes approximately 60 minutes for the balloon to reach 100 mb. During its ascent, the balloon drifted as much as 80 km from its launch site. However, no corrections for time and balloon drift were made in this study. Both the upper-air data and hourly surface were available from the McIDAS system at AFGL. For most soundings, significant level and mandatory level data were available. The significant level thermodynamic data were reports at pressure levels, whereas, the significant level wind data were reports at height levels. First of all, we combined mandatory level and significant level thermodynamic data and then interpolated temperature and dew point temperature into 25 mb intervals using a cubic spline under tension curve fitting technique (Cline, 1973). The pressure level for each significant wind datum was interpolated from the height data reported at the mandatory level. Then we combined the mandatory level and significant level wind data and interpolated the zonal (u) and meridional (southerly) (v) wind components into 25 mb intervals. The geopotential height at each 25 mb interval was calculated from temperature and dew point using the hydrostatic assumption.

The thermodynamic and wind data for each pressure surface were next interpolated onto a 4 x 2 degree coarse grid from 100 degrees W to 80 degrees W and 35 degrees N to 45 degrees N using Cressman's (1959) objective analysis scheme. The scan radii were 3.0d, 2.0d, 1.5d, 1.3d, 1.2d, 1.1d, with [d] equal to the mean station separation, which is approximately 300 to 400 km. We further interpolated the data from the coarse grid into a 2 x 1 degree fine grid using cubic spline under tension. Thus, the objective analysis scheme was essentially the same as that which was used earlier by Ogura and Chen (1977) and Ogura et al., (1979). It is important to note that to interpolate the data onto a fine grid does not reduce the resoluble scale, which is determined by the station separation of the observations. The scale of analyses depend on the original observations rather that the grid system chosen. It is not possible to resolve signals with wavelengths smaller than the mean station separation. The purpose of the interpolation onto the fine grid was to provide a denser grid for the finite difference calculation of horizontal derivatives of variables such as divergence and the vertical component of vorticity.

1. INTRODUCTION

Numerical simulations of cloud development under large-scale lifting were made by Chang and Orville (1973). In their simulations, a cloud developed to a height of 8 km after 2 hrs with a low-level lifting of 5 cm sec^{-1} at 1 km. In another case, when the lifting was removed, all clouds stayed below the 2 km level. Cotton et al., (1976) tried to make joint use of a sea breeze model (Pielke, 1974) and a cloud model (Cotton, 1975) to produce some observed showers in Florida. They illustrated the dramatic effects of the perturbed sounding and formation of regions of horizontal convergence due to the sea breeze circulation on the development of a cloud. Soong and Ogura (1980) have proposed a cloud ensemble model on which the large-scale forcing can be imposed. Recent work by Soong and Tao (1980) and Wang (1984) have suggested that in doing numerical simulations of observed cloud activity, the incorporation of large-scale forcing in some way is a necessity.

Adiabatic cooling due to large-scale lifting usually leads to the formation of clouds and precipitation systems. Small scale updrafts and downdrafts are normally found in clouds and precipitation systems with large-scale ascent. The large scale lifting is small and, in general, on the order of several centimeters per second. Two methods are frequently used to compute large-scale vertical velocities from observed upper-air data (Panofsky, 1946); these are the adiabatic and the kinematic methods. The first is based on the assumption that changes of state of atmospheric air are adiabatic, and the second depends on the principle of mass continuity.

In this study, the environmental conditions as well as large-scale lifting for two snowstorm cases during SNOW TWO, 16-17 January and 23-24 January 1984, were studied. Since the adiabatic assumption may not be a good assumption during a period of snowstorm activity (due to the effects of latent heat release and convective transports as a result of convective overturning), the kinematic method was used to compute large-scale vertical motion in this study. The large-scale vertical motion computed, as well as environmental conditions studied for both cases, will provide useful information for the proper choice of initial conditions for our numerical simulations of cloud development in the future.

2. DATA SOURCES AND METHODS OF ANALYSIS

Surface observations and upper-air rawinsonde measurements taken at SNOW TWO/Smoke Week VI at Camp Grayling, MI were received from the Cold Regions Research and Engineering Laboratory, Corps of Engineers, Hanover, New Hampshire. Surface charts and constant pressure surface charts from Air Force Systems Command Headquarters, Andrews AFB,

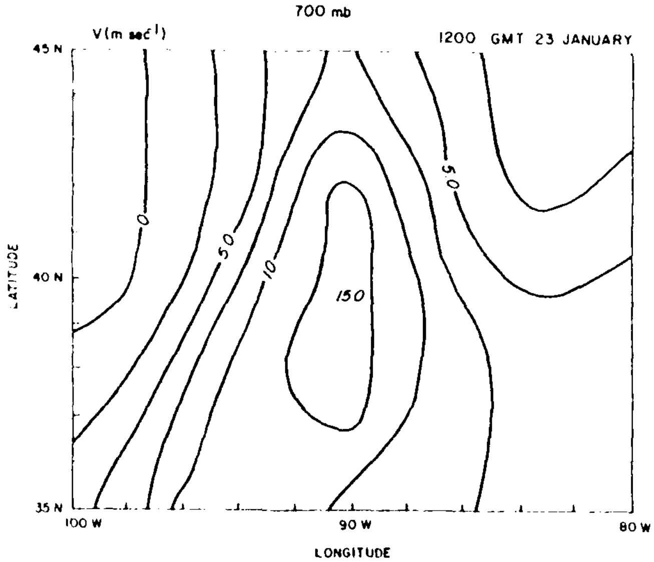

Figure 14. Horizontal Distributions of Meridional Wind at the 700 mb Level for 1200 GMT on 23 January 1984.

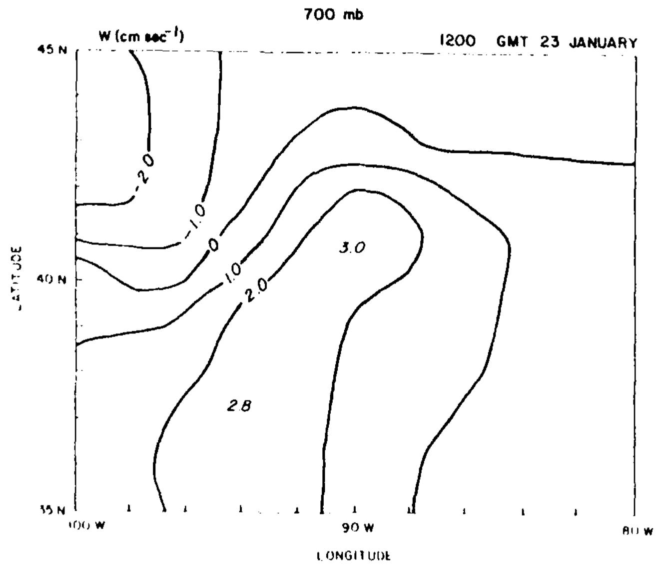

Figure 15. Horizontal Distributions of Vertical Velocity at the 700 mb Level for 1200 GMT on 23 January 1984.

As the surface trough moved eastward, the convective activity propagated eastward and moved out of the central United States. One day later the vertical cross sections of meridional wind and vertical motion (Figures 16 & 17) show that both regions of upward motion and strong southerly wind moved to the eastern boundary of the domain. Subsidence was found in the Central United States where the convection was suppressed. Thus, the computed vertical motion agreed well with the observed convective activity.

The axis of coldest cloud top temperatures entered southwestern Michigan at approximately 1400 GMT 23 January, extending northward and occupied most of Michigan at 1700 GMT (Figures 18 & 19). The NWS (National Weather Service) regular upper-air observations with 12 hr intervals were apparently not sufficient to resolve the changes in detail during the passage of this weather system at Michigan. Fortunately, an upper-air observation at Camp Grayling was available at 1530 GMT. The time changes of the atmospheric structure at Camp Grayling will be described later. The vertical cross sections at 1200 GMT 23 January and 0000 GMT 24 January representing the situations before and after the passage of this weather system at Michigan will be presented using rawinsonde data from stations near 44 degrees N. The stations used were:

Huron, SD (98.2 degrees W, 44.4 degrees N),
St. Cloud, MN (94.2 degrees W, 45.6 degrees N),
Green Bay, WI (88.1 degrees W, 44.5 degrees N),
Flint, MI (83.7 degrees W, 43.0 degrees N),
Buffalo, NY (78.7 degrees W, 42.9 degrees N),
Albany, NY (73.8 degrees W, 42.8 degrees N).

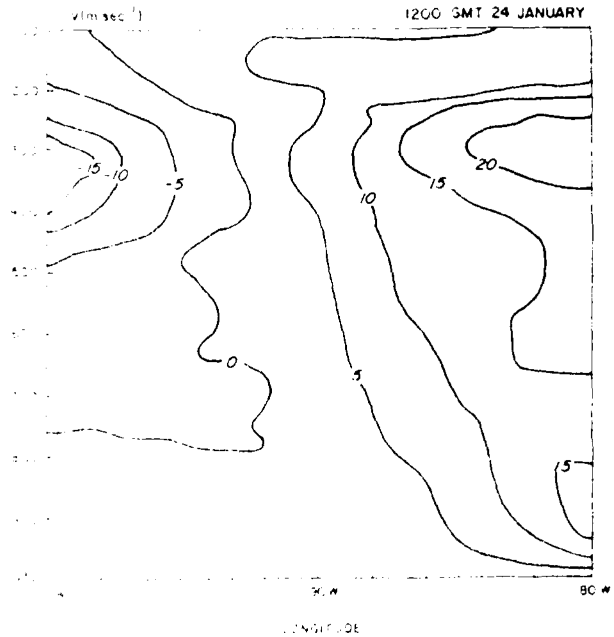

Fig... ...(?) Vertical, West-East Cross Sections of Meridional Wind Averaged from 40 degrees N through 42 degrees N for 1200 GMT on 24 January 1984.

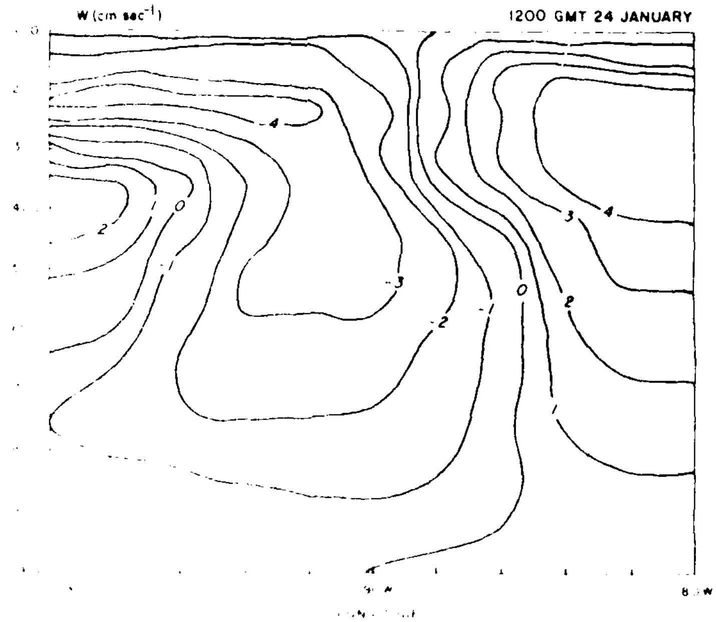

... East Cross Sections of Vertical Velocity ... 40 degrees N through 42 degrees N for 1200 GMT ... 1984.

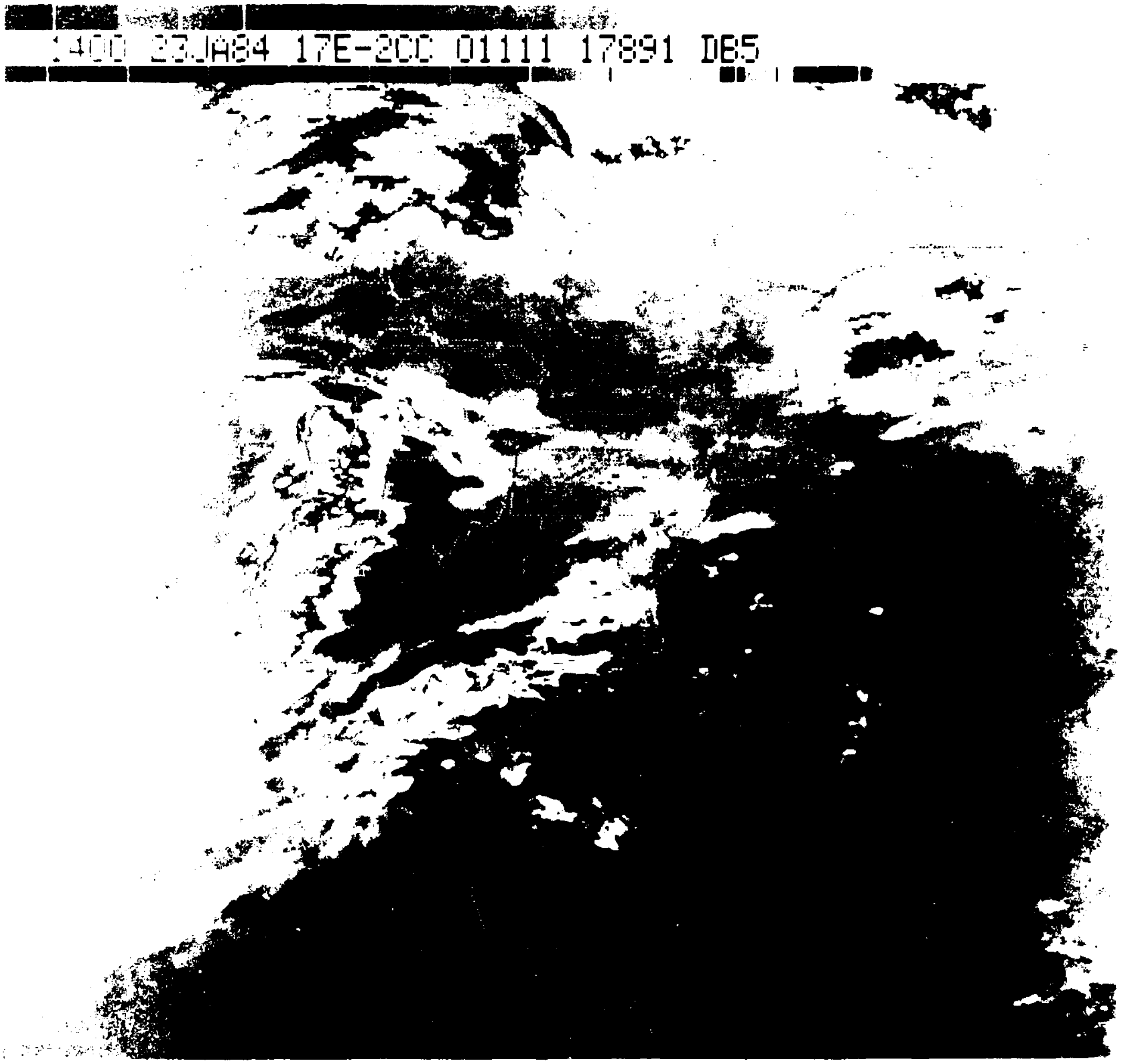

Figure 18. GOES-East Infrared Pictures of the Eastern United States at 1400 GMT on 23 January 1984.

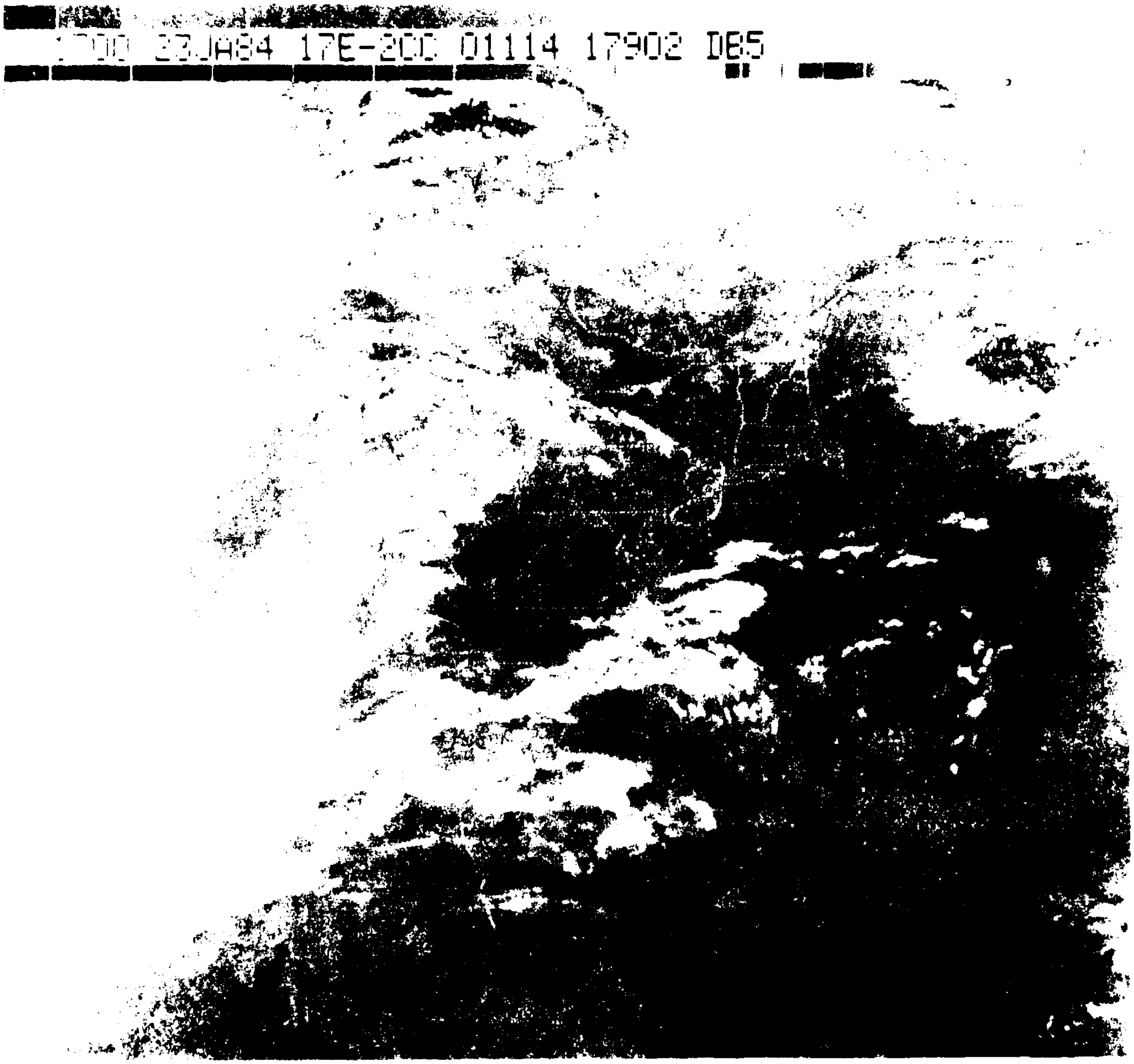

Figure 19. GOES-East Infrared Pictures of the Eastern United States at 1700 GMT on 23 January 1984.

At 1200 GMT 23 January, the vertical cross section of meridional wind shows southerly flow in the central United States with slightly warmer potential temperature and equivalent potential temperature in the low levels (Figures 20 & 21). The vertical cross section of relative humidity (Figure 23) also shows that the moisture was mainly confined to the low levels. It is interesting to note that the meridional wind shown in Figure 22 was much weaker than that at 41 degrees N which resulted from objective analysis (Figure 9). The horizontal distribution of meridional wind shown in Figure 14 resulting from the objective analysis did show the decrease of the wind speed toward the north together with decreasing dew point temperature at 1200 GMT (Figure 13). Recall from the GOES-East satellite data indicates that the major convective activity prior to 1200 GMT was mainly located south of Lake Michigan. As the trough intensified and moved eastward, the area of deep convection extended northward. Twelve hours later (0000 GMT 24 January) the meridional flow along the cross section increased drastically and reached as high as 25 m sec^{-1} at Flint, MI at 900 mb and over 40 m sec^{-1} at high levels (Figure 26). Accompanying the strengthening in the southerly wind, the low level potential temperature and equivalent potential temperatures also increased considerably (Figures 24 & 25). A conditionally unstable layer (where θ_e decreases with height) was found between 700 mb and 500 mb at Flint, MI. The cross section of relative humidity indicates the development of deep clouds (Figure 27) near the axis of maximum southerly wind, which is consistent with the satellite observations. These results suggested that the strengthening of the southerly flow resulting from the development of the trough brought in the warm and moist air and may have played an important role in the formation of deep convection.

The correlation between the surface convergence computed from the hourly surface data and the region of cold cloud top temperature was poor (not shown). The close relationship between the low-level convergence and the convective activities found by Ogura et al., (1979) and others during the GARP (Global Atmospheric Research Program) Atlantic Tropical Experiment was not evident for this winter snowstorm case. In the Tropics, the atmosphere is conditionally unstable. A minimum of equivalent potential temperature exists at 700 mb. The low-level convergence provides the moisture supply and the lifting required for the release of potential instability. However, for the 23-24 January snowstorm case, the equivalent potential temperature in the low troposphere was considerably colder than in the mid-troposphere and high levels. It was, therefore, unlikely for the air parcel in the low levels to grow and develop into a tall cloud. It appears that the low-level convergence was not important for the development of deep clouds for this case.

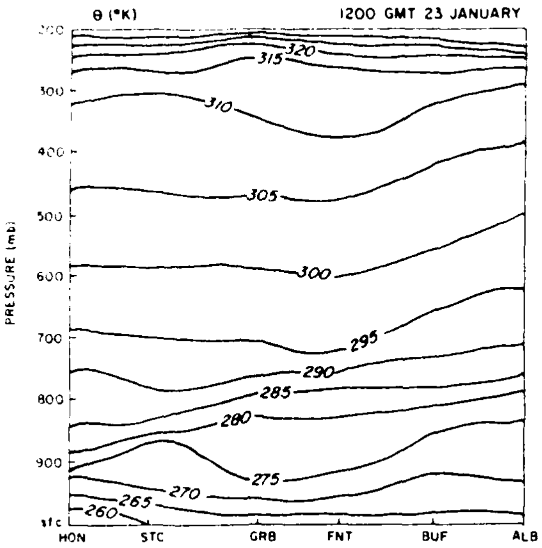

Figure 20. Vertical Cross Sections of Potential Temperature through Huron, SD (HON), St. Cloud, MN (STC), Green Bay, WI (GRB), Flint, MI (FNT), Buffalo, NY (BUF), and Albany, NY (ALB) at 1200 GMT on 23 January 1984. Shaded areas represent relative humidities greater than 90%.

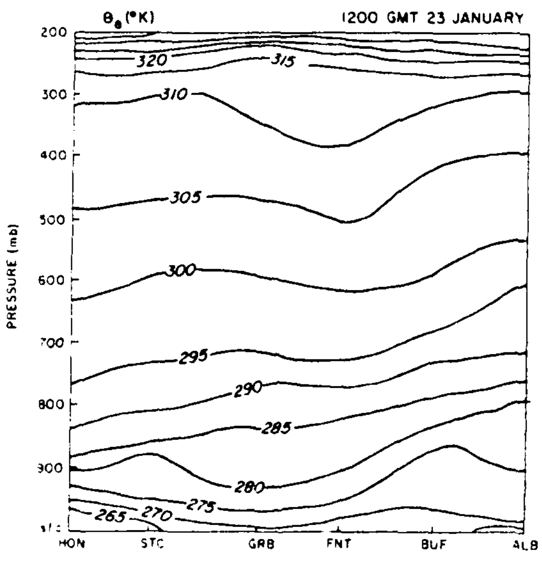

Figure 21. Vertical Cross Sections of Equivalent Potential Temperature through Huron, SD (HON), St. Cloud, MN (STC), Green Bay, WI (GRB), Flint, MI (FNT) Buffalo, NY (BUF), and Albany, NY (ALB) at 1200 GMT on 23 January 1984. Shaded areas represent relative humidities greater than 90%.

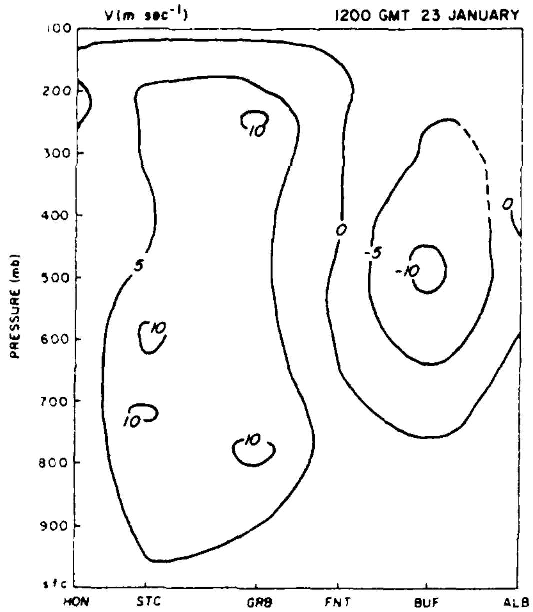

Figure 22. Vertical Cross Sections of Meridional Wind through Huron, SD (HON), St. Cloud, MN (STC), Green Bay, WI (GRB), Flint, MI, Buffalo, NY (BUF), and Albany, NY (ALB) at 1200 GMT on 23 January 1984. Shaded areas represent relative humidities greater than 90%.

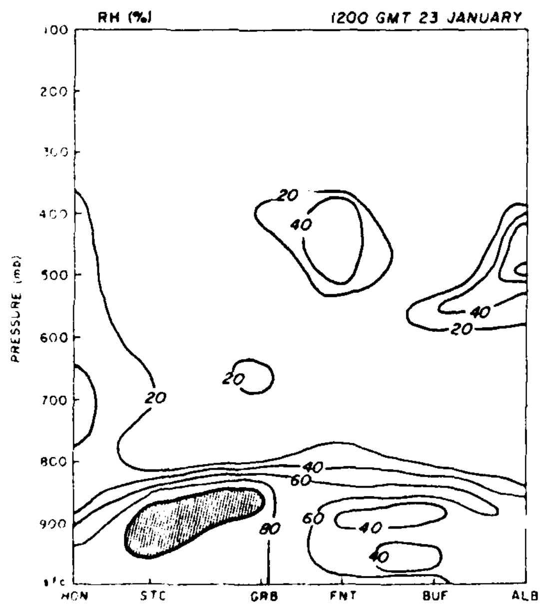

Figure 23. Vertical Cross Sections of Relative Humidity through Huron, SD (HON), St. Cloud, MN (STC), Green Bay, WI (GRB), Flint, MI (FNT), Buffalo, NY (BUF), and Albany, NY (ALB) at 1200 GMT on 23 January 1984. Shaded areas represent relative humidities greater than 90%.

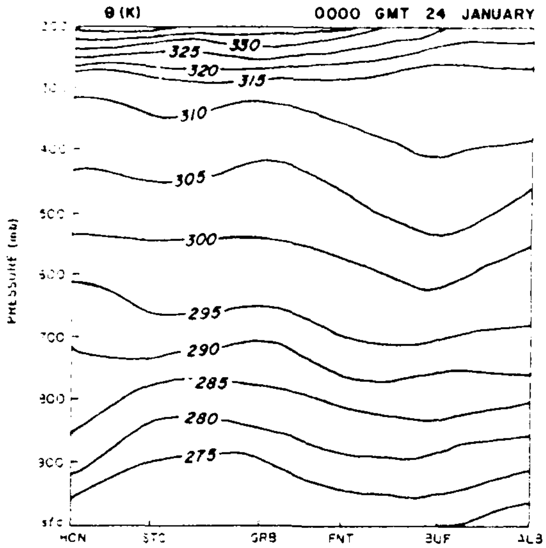

Figure 24. Vertical Cross Sections of Potential Temperature through Huron, SD (HON), St. Cloud, MN (STC), Green Bay, WI (GRB), Flint, MI (FNT), Buffalo, NY (BUF), and Albany, NY (ALB) at 0000 GMT on 24 January 1984. Shaded areas represent relative humidities greater than 90%. Lines are dashed in regions where data are missing.

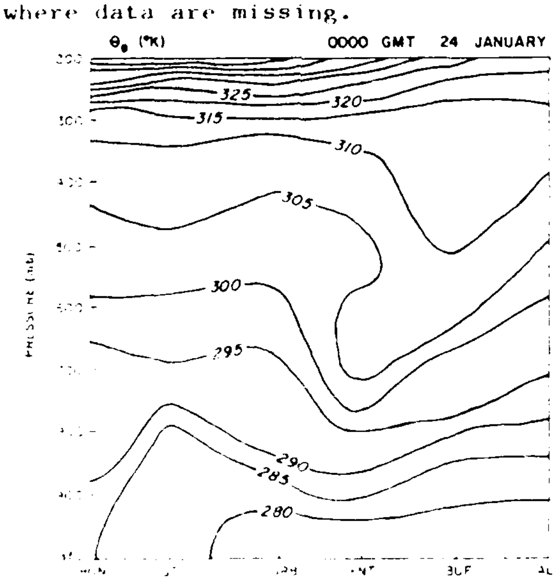

Figure 25. Vertical Cross Sections of Equivalent Potential Temperature through Huron, SD (HON), St. Cloud, MN (STC), Green Bay, WI (GRB), Flint, MI (FNT), Buffalo, NY (BUF), and Albany, NY (ALB) at 0000 GMT on 24 January 1984. Shaded areas represent relative humidities greater than 90%. Lines are dashed in regions where data are missing.

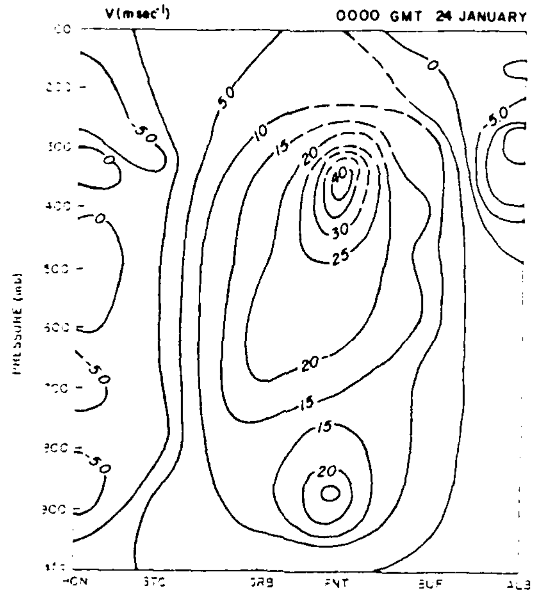

Figure 26. Vertical Cross Sections of Meridional Wind through Huron, SD (HON), St. Cloud, MN (STC), Green Bay, WI (GRB), Flint, MI (FNT), Buffalo, NY (BUF), and Albany, NY (ALB) at 0000 GMT on 24 January 1984. Shaded areas represent relative humidities greater than 90%. Lines are dashed in regions where data are missing.

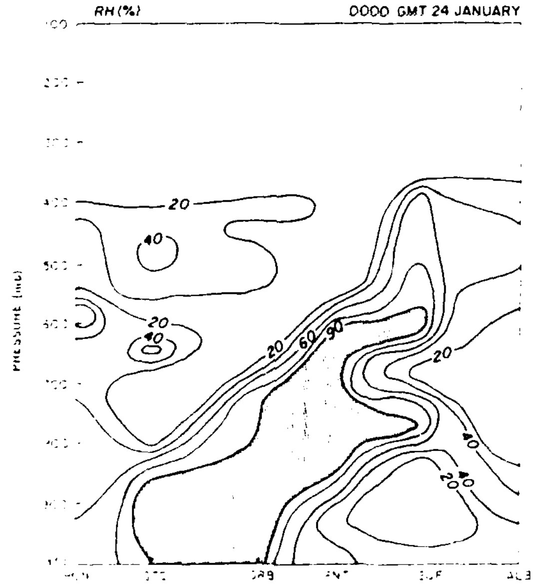

Figure 27. Vertical Cross Sections of Relative Humidity through Huron, SD (HON), St. Cloud, MN (STC), Green Bay, WI (GRB), Flint, MI (FNT), Buffalo, NY (BUF), and Albany, NY (ALB) at 0000 GMT on 24 January 1984. Shaded areas represent relative humidities greater than 90%. Lines are dashed in regions where data are missing.

3.3 Time Series of Rawinsonde Observations at Camp Grayling

Rawinsonde launches were made on site at 0500 GMT, 1530 GMT 23 January and 0500 GMT 24 January representing the conditions before, during, and after the passage of the convective system, respectively. Figures 28, 29, 30, and 31 shows the vertical profiles of zonal wind, meridional wind, potential temperature, and equivalent potential temperature in time series. The zonal wind (Figure 28) shows slight changes between 0500 GMT and 1530 GMT 23 January, however, drastic changes in the meridional wind were evident (Figure 29). The meridional wind was rather weak at 0500 GMT. It increased to 20 m sec^{-1} for most levels above 900 mb. Three hours earlier, a nearby station, Flint, MI, only reported a meridional wind as strong as 10 m sec^{-1} (Figure 22). It was clear that the strong meridional wind and the intense convective activity both occurred after 1200 GMT 23 January at Camp Grayling. Warming below 700 mb between 0500 GMT and 1530 GMT was clearly shown from the vertical profiles of potential temperature (Figure 30). The increase in the equivalent potential temperature (Figure 31) between 0500 GMT and 1530 GMT is very striking. Above 700 mb, the atmosphere would have become unstable at 1530 GMT if the latent heat release by ice process had been considered. Thus, the inflow of moist and warm air from the south created favorable conditions for the development of deep convection. Tall clouds would have developed if large-scale lifting was present above 700 mb. It appears that the relatively strong convergence (Figure 10) and the large-scale lifting (Figure 11) in the mid-troposphere were very important for the release of potential instability for this case.

At 0500 GMT 24 January, after the passage of the convective system, the meridional wind weakened and both the potential temperature and equivalent potential temperature decreased except below 900 mb. An inversion at 825 mb with a well mixed layer was found. Since the air above the inversion was relatively dry, this inversion was possibly caused by the subsidence which prevailed behind the meridional wind maximum.

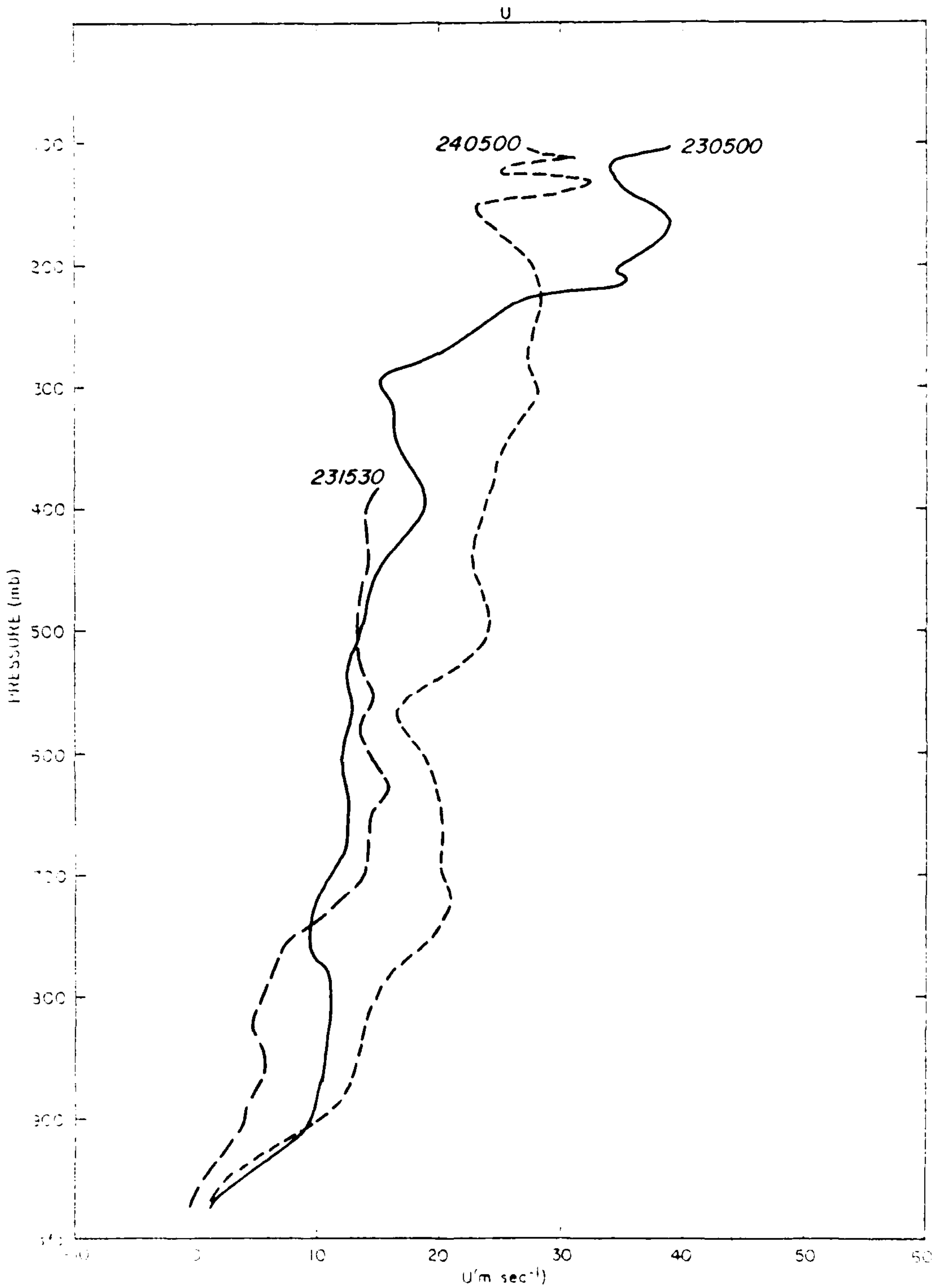

[illegible]8. Vertical Profiles of Zonal Wind at Camp Grayling, MI at 0500 GMT 23 January, (230500), 1530 GMT 23 January (231530), and 0500 GMT 24 January (240500) 1984.

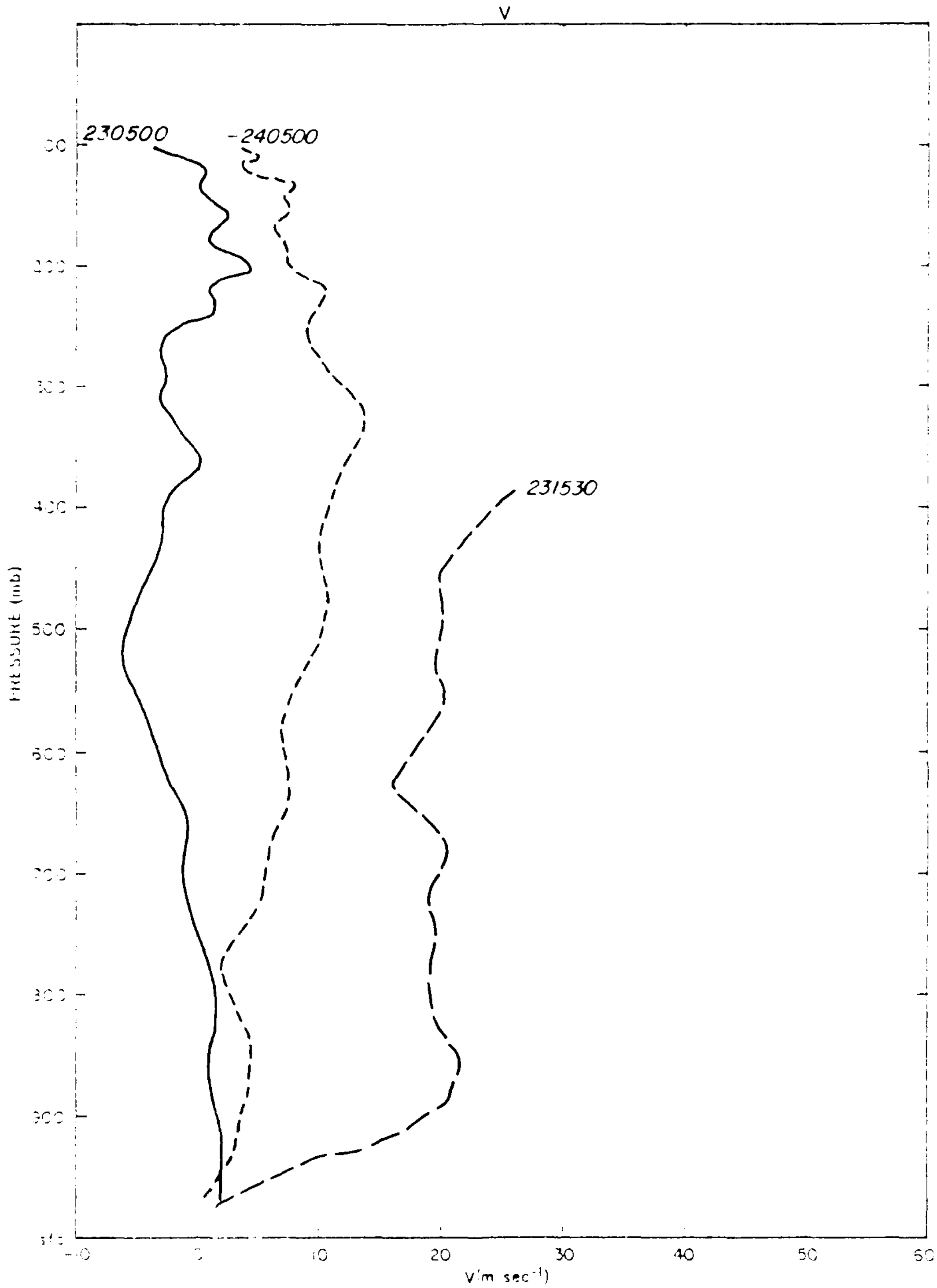

Figure 29. Vertical Profiles of Meridional Wind at Camp Grayling, MI at 0500 GMT 23 January, (230500), 1530 GMT 23 January (231530), and 0500 GMT 24 January (240500) 1984.

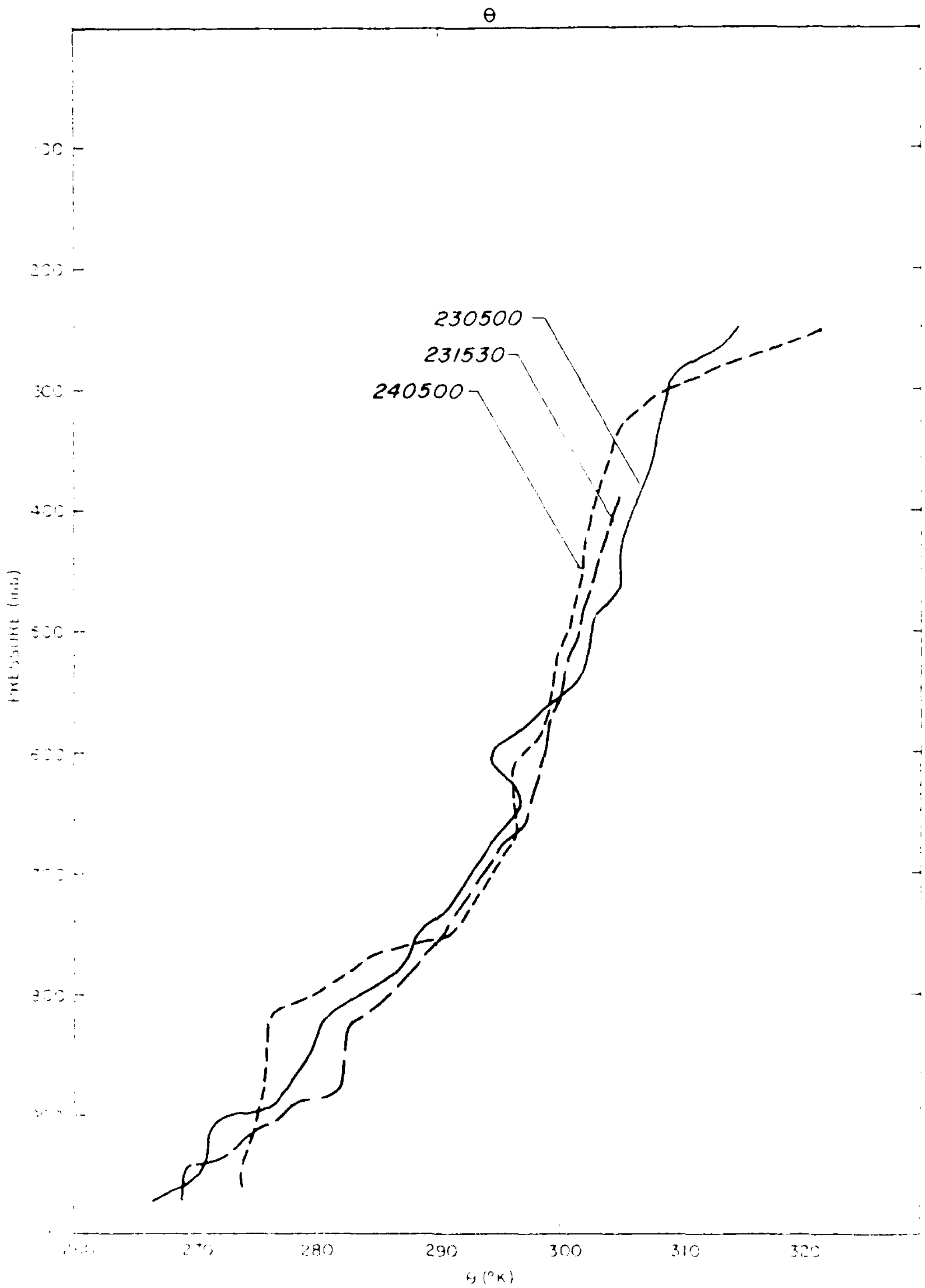

[illegible] Potential Temperature at Camp Grayling, [illegible] GMT 23 January, (230500), 1530 GMT 23 January [illegible] 0500 GMT 24 January (240500) 1984.

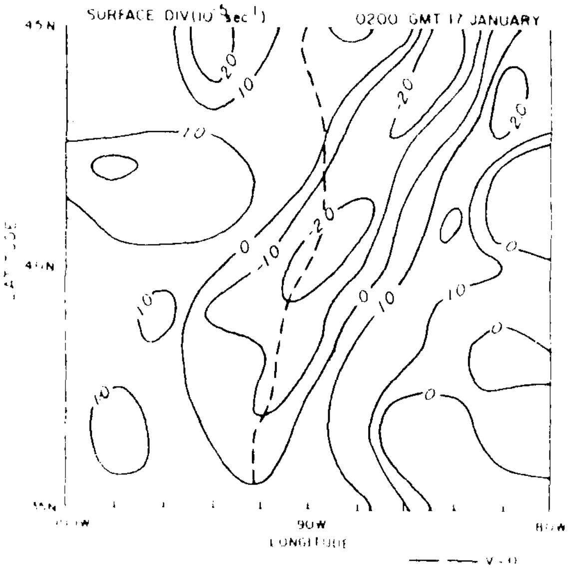

Figure [illegible]. Surface Divergence Fields for 0200 GMT 17 January 1984. Dashed line indicates the isoline where the meridional wind is zero.

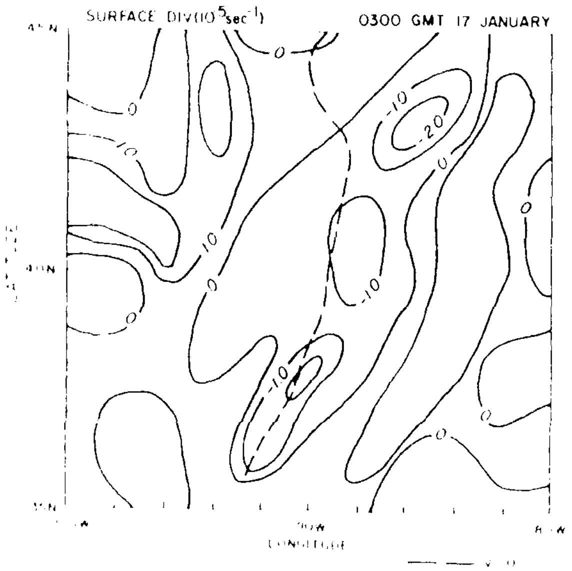

Figure [illegible]. Surface Divergence Fields for 0300 GMT 17 January 1984. Dashed line indicates the isoline where the meridional wind is zero.

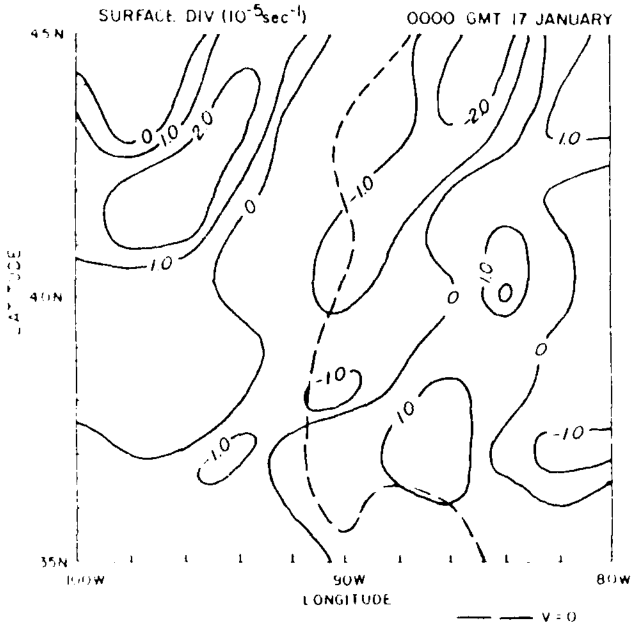

Figure 46. Surface Divergence Fields for 0000 GMT 17 January 1984. Dashed line indicates the isoline where the meridional wind is zero.

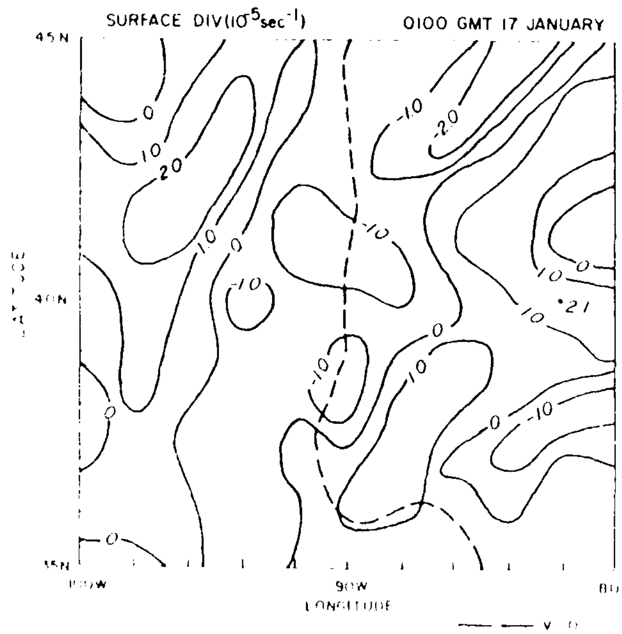

Figure 47. Surface Divergence Fields for 0100 GMT 17 January 1984. Dashed line indicates the isoline where the meridional wind is zero.

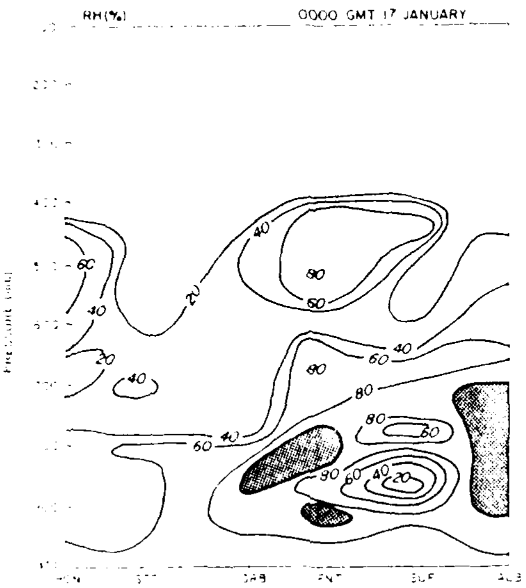

[illegible] Vertical Cross Sections of Relative Humidity through Huron, SD (HON), St. Cloud, MN (STC), Green Bay, WI (GRB), Flint, MI (FNT), Buffalo, NY (BUF), and Albany, NY (ALB) at 0000 GMT on 17 January 1984. Shaded areas represent relative humidities greater than 90%. Lines are dashed in regions where data are missing.

[illegible] Surface Analysis

[illegible] surface convergence between 2300 GMT 16 January and [illegible] January are shown in Figures 45, 46, 47, 48, and 49. The [illegible] the meridional wind vanished was also indicated. It is [illegible] that the surface convergence zone was located over the frontal [illegible]

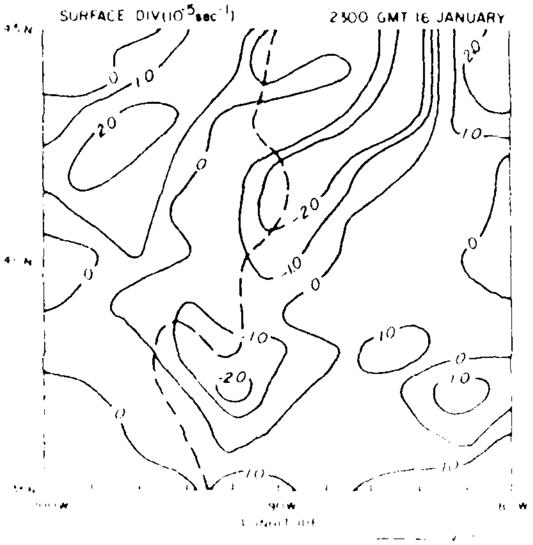

[illegible] Surface Divergence Fields for 2300 GMT 16 January 1984. [illegible] indicates the isoline where the meridional wind [illegible]

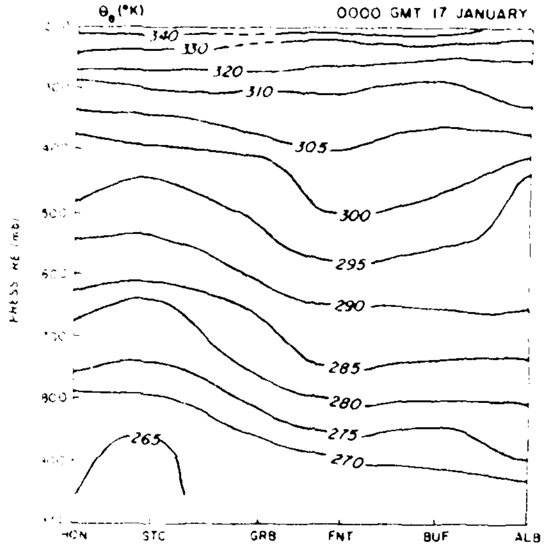

Figure 42. Vertical Cross Sections of Equivalent Potential Temperature through Huron, SD (HON), St. Cloud, MN (STC), Green Bay, WI (GRB), Flint, MI (FNT), Buffalo, NY (BUF), and Albany, NY (ALB) at 0000 GMT on 17 January 1984. Shaded areas represent relative humidities greater than 90%. Lines are dashed in regions where data are missing.

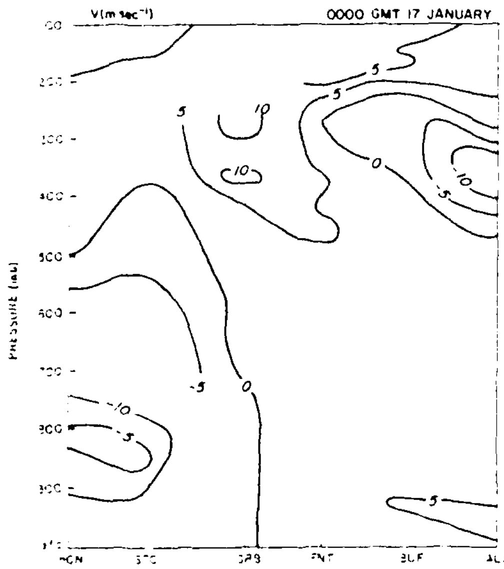

Figure 43. Vertical Cross Sections of Meridional Wind through Huron, SD (HON), St. Cloud, MN (STC), Green Bay, WI (GRB), Flint, MI (FNT), Buffalo, NY (BUF), and Albany, NY (ALB) at 0000 GMT on 17 January 1984. Shaded areas represent relative humidities greater than 90%. Lines are dashed in regions where data are missing.

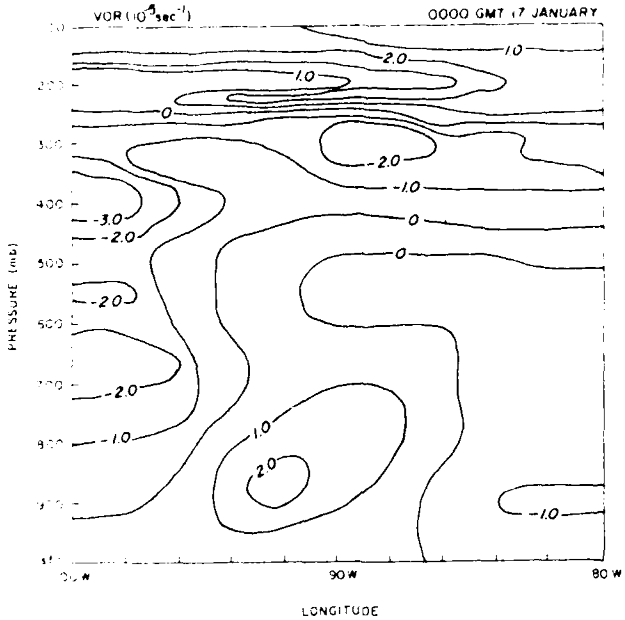

Figure 4. Vertical, West-East Cross Sections of Relative Vorticity Averaged from 40 degrees N through 42 degrees N for 0000 GMT on 17 January 1984.

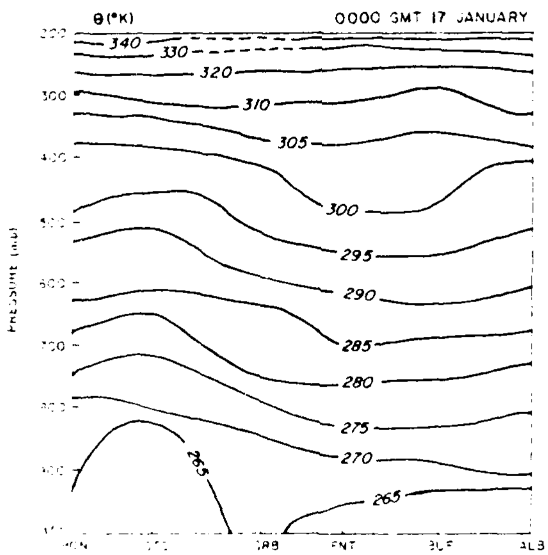

Vertical Cross Sections of Potential Temperature through Huron, SD (HON), St. Cloud, MN (STC), Green Bay, WI (GRB), Flint, MI (FNT), Buffalo, NY (BUF), and Albany, NY (ALB) at 0000 GMT on 17 January 1984. Shaded areas represent relative humidities greater than 90%. Lines are dashed in regions where data are missing.

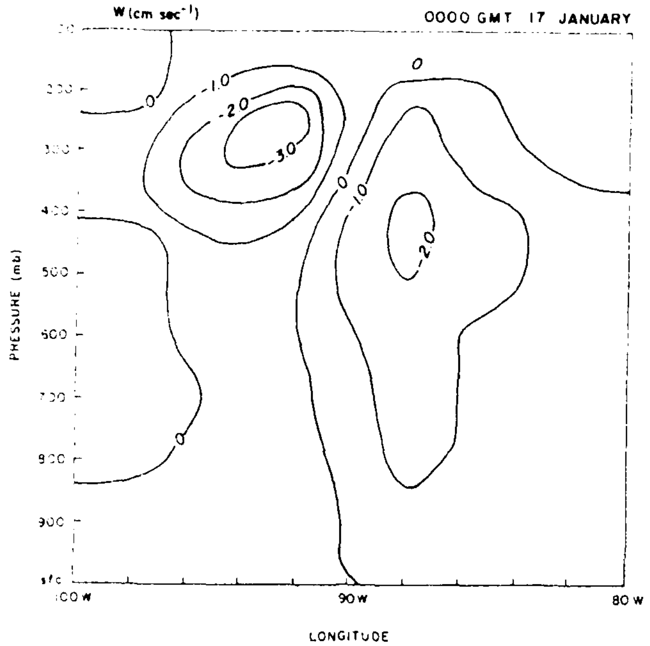

Figure 38. Vertical, West-East Cross Sections of Vertical Velocity averaged from 40 degrees N through 42 degrees N for 0000 GMT on 17 January 1984.

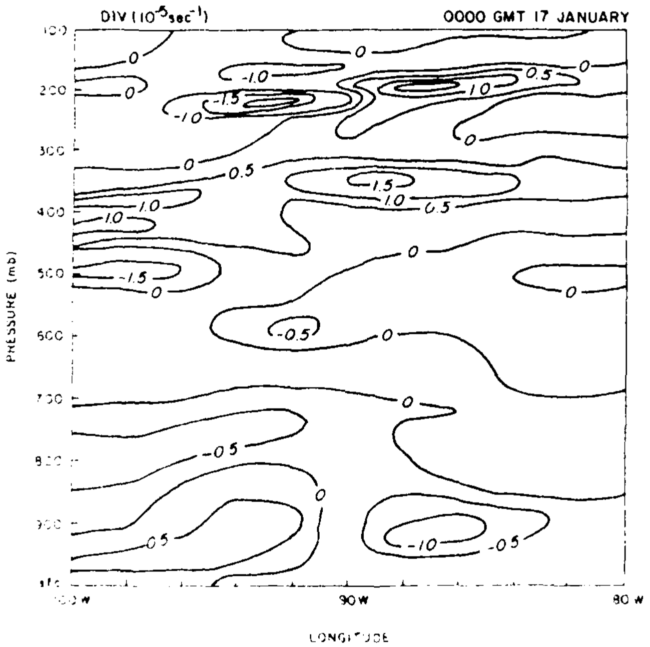

Figure 39. Vertical, West-East Cross Sections of Divergence averaged from 40 degrees N through 42 degrees N for 0000 GMT on 17 January 1984.

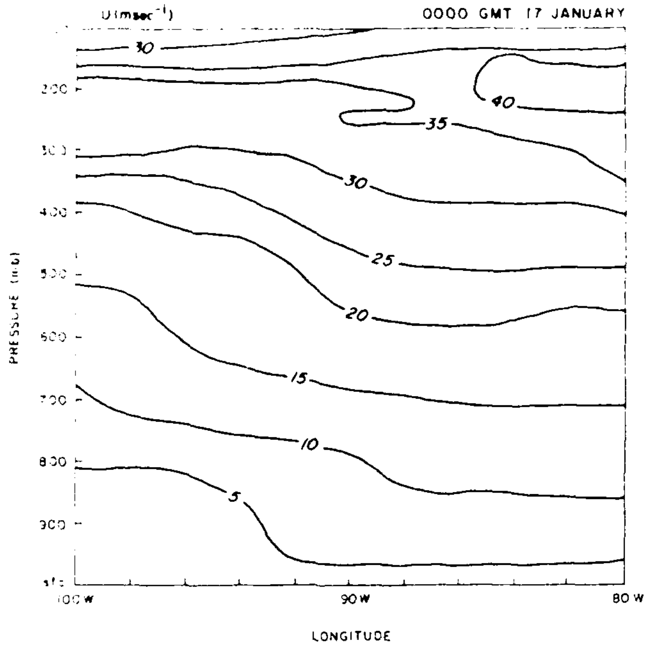

Figure 36. Vertical, West-East Cross Sections of Zonal Wind Averaged from 40 degrees N through 42 degrees N for 0000 GMT on 17 January 1984.

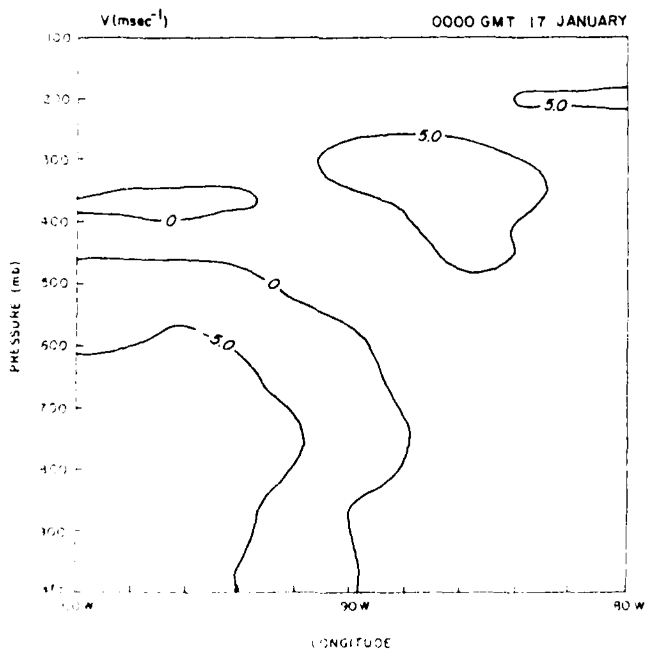

Figure 37. Vertical, West-East Cross Sections of Meridional Wind Averaged from 40 degrees N through 42 degrees N for 0000 GMT on 17 January 1984.

4.2 Results of Upper-Air Data Analyses

The west-east cross sections averaged between 40 degrees to 42 degrees for zonal wind, meridional wind, divergence, vertical motion, and the vertical component of relative vorticity for 0000 GMT 17 January are shown in Figures 36, 37, 38, 39, and 40. The speed of the zonal current was comparable to the 23-24 January case (Figure 36). However, the strong meridional wind was not found in the region of maximum cloud activities. Southerly wind was found east of 90 degrees W with northerly wind west of it below 500 mb indicating the presence of a frontal discontinuity (Figure 37). Upward motion was found over the frontal zone coinciding with the area of maximum cloud activities observed by satellite visible image (Figure 38). The region of strongest upward motion was located slightly ahead of the surface cold front with a maximum of 1.3 cm sec^{-1} at 750 mb and a maximum of 2.4 cm sec^{-1} at 400 mb. Sinking motion was computed behind the cold front in agreement with the clear sky observed by satellite visible picture. The sinking motion behind the cold front was also observed by Ogura and Portis (1982) for a cold front passing through the central United States in April 1979. In the region of upward motion, convergence with a magnitude of $-1.1 \times 10^{-5} sec^{-1}$ at 900 mb was evident with weak convergence in the mid-troposphere (Figure 38). The divergence associated with the outflow layer was found mainly between 300 and 400 mb. Consequently the maximum vertical motion in the upper troposphere was located at 400 mb which was 100 mb lower than the 23-24 January case (Figures 11 & 38). This is consistent with the satellite IR cloud top temperatures observed by both cases. Satellite observations showed that the 23-24 January case had colder cloud top temperatures than the 16-17 January case. A weak divergence layer between 600-800 mb was also present in the area of rising motion. The vertical cross section of the vertical component of relative vorticity shows maximum cyclonic vorticity in the lower troposphere over the frontal zone (Figure 40).

The vertical cross sections of potential temperature, equivalent potential temperature, meridional wind and relative humidity constructed from six rawinsonde stations near 44 degrees N are shown in Figures 41, 42, 43 and 44. Sharp horizontal gradients of potential temperature and equivalent potential temperatures were found between Green Bay, WI (88.1 degrees W, 44.5 degrees N) and St. Cloud, MN (94.2 degrees W, 45.6 degrees N) in the low troposphere due to the presence of the cold front (Figures 41 & 42). The air ahead of the cold front was relatively warmer and had a higher moisture content (Figure 44). A moist layer ahead of the cold front was also present in the middle layer. It is important to note that the atmosphere was stable both ahead and over the frontal zone. As the cold front moved eastward, the relatively warm and moist air ahead of the cold front was lifted and may have become saturated and produced clouds and precipitation. The low level meridional wind maximum which was evident ahead of the surface trough for 23-24 January case was not found for this case. The meridional wind was weak in general (Figure 43).

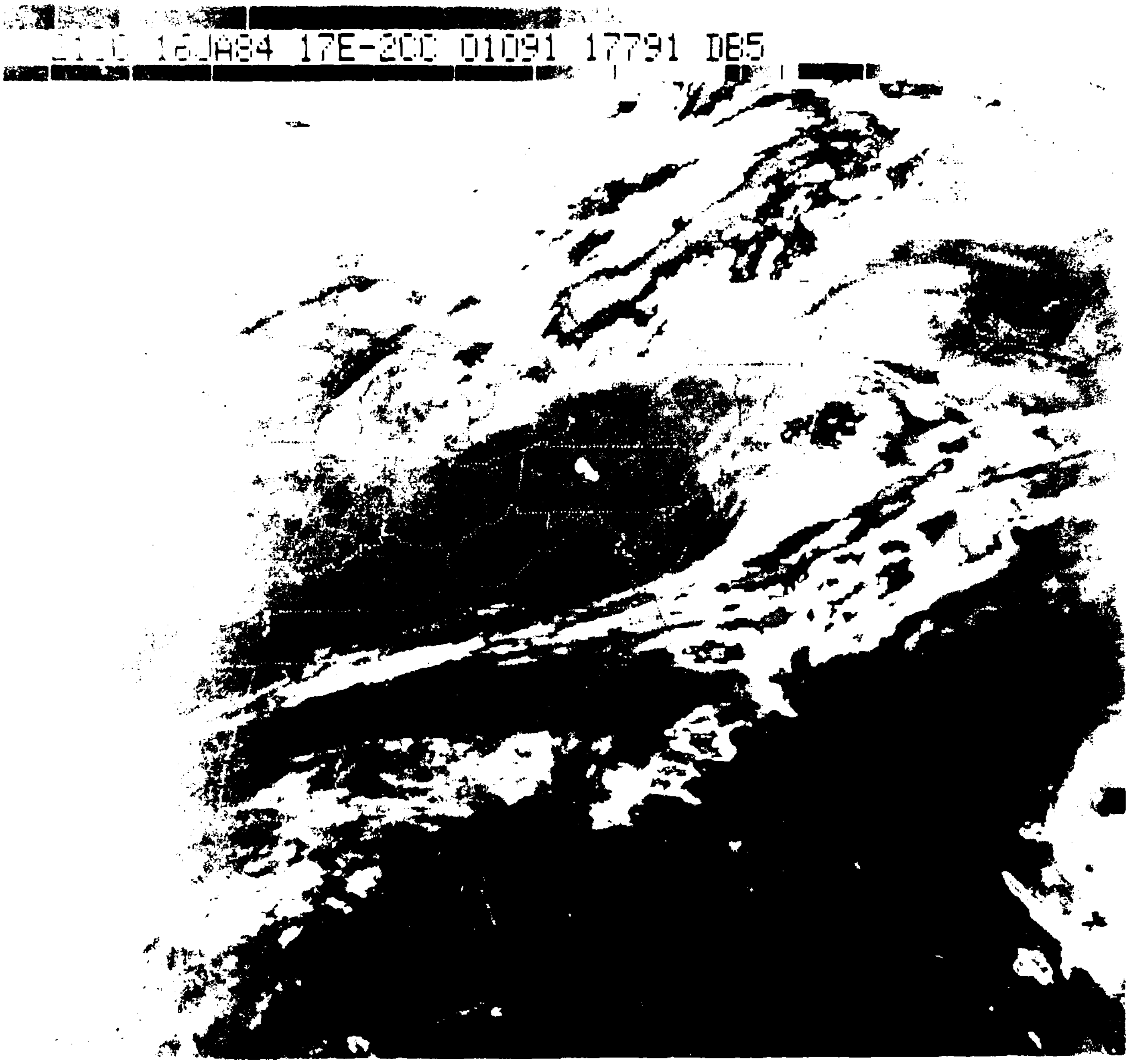

Figure 35. GOES-East Infrared Picture of the Central United States for 2100 GMT on 16 January 1984.

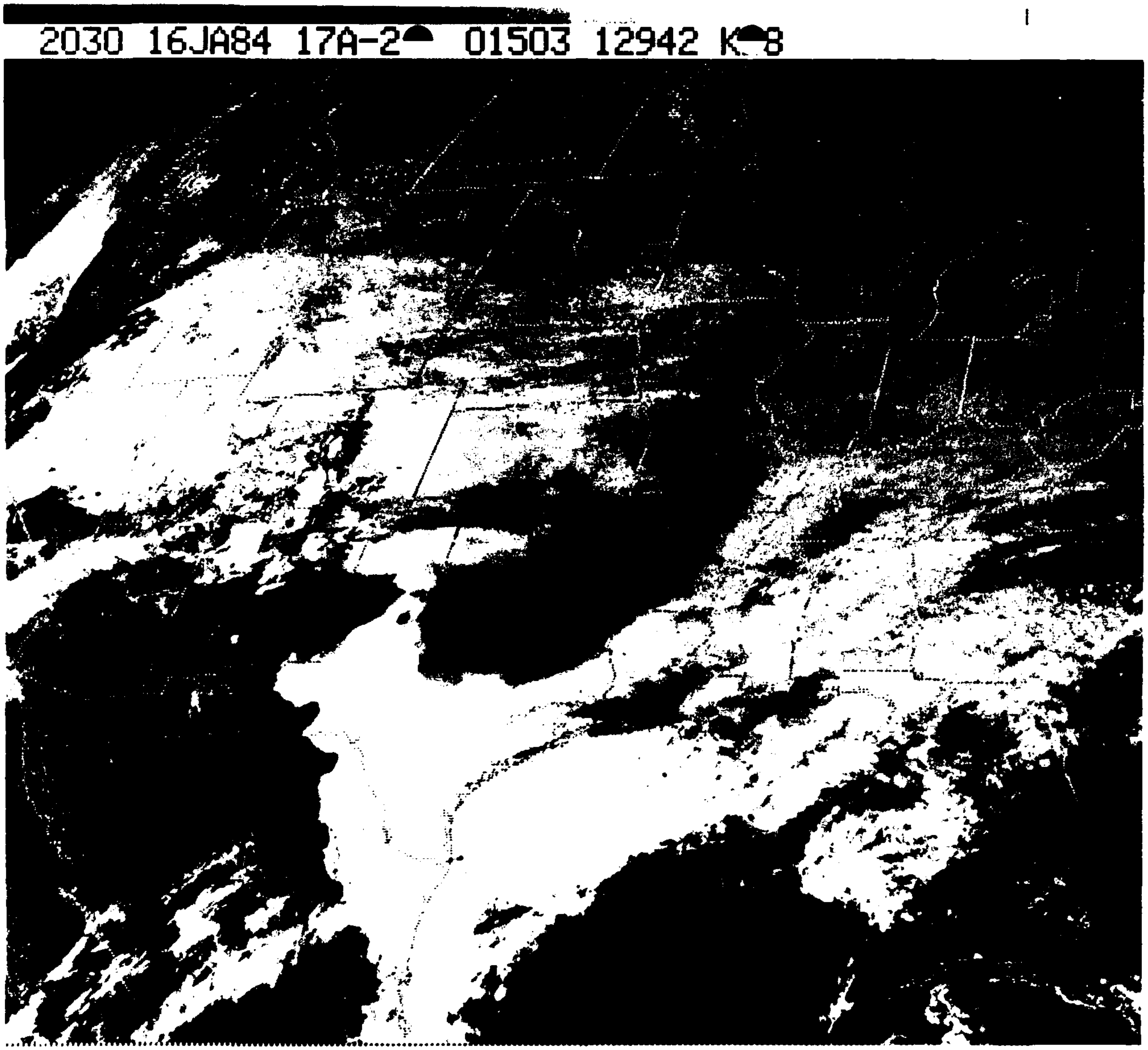

Figure 34. GOES-East Visible Picture of the Central United States for 2030 GMT on 16 January 1984.

4. CASE OF 16-17 JANUARY

4.1 Synoptic Situation

A cold front was found extending from northern Canada to the United States/Canadian border north of Montana at 1200 GMT 15 January (not shown). The cold arctic air behind the cold front and the cold front moved southward gradually and intruded into the northwest United States. At 0000 GMT 17 January the 500 mb weather chart (Figure 32) shows a low pressure center located over northern Canada, with a surface cold front extending southwestward into the central United States and northwestward from Oklahoma to Washington (Figure 33). Behind the surface front a weak high pressure center was situated over Nebraska. A frontal cloud band began to form near 1500 GMT 16 January and became well organized at [illegible] GMT 16 January (Figure 34) as the front moved southwestward. This cloud band extended from Illinois to Texas. Although the GOES-East visible image at 2030 16 January shows convective activity over most of the eastern United States, the GOES-East infrared picture at 2100 GMT (Figure 35) indicated that the cloud top temperatures were considerably warmer than the 23-24 January case. Only a narrow cold cirrus cloud band extending from Nebraska to southern Michigan and scattered cirrus clouds over the boundaries between Illinois, Kentucky, and Missouri were present. Behind the surface cold front the weak high pressure system produced clear sky. In the southeast, cloudiness associated with a [illegible] was also evident.

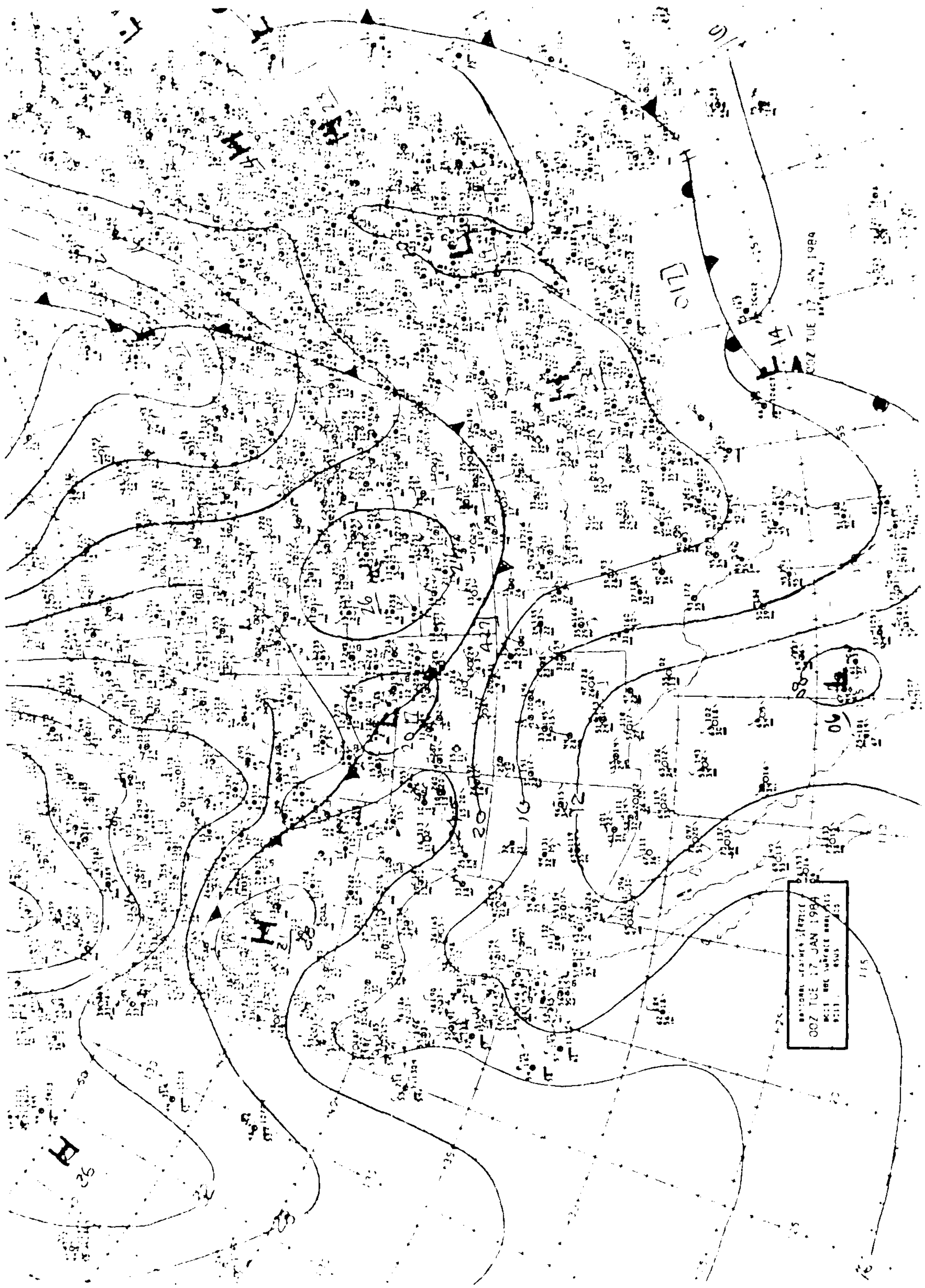

Figure [illegible]. Surface Chart at 0000 GMT on 17 January 1984.

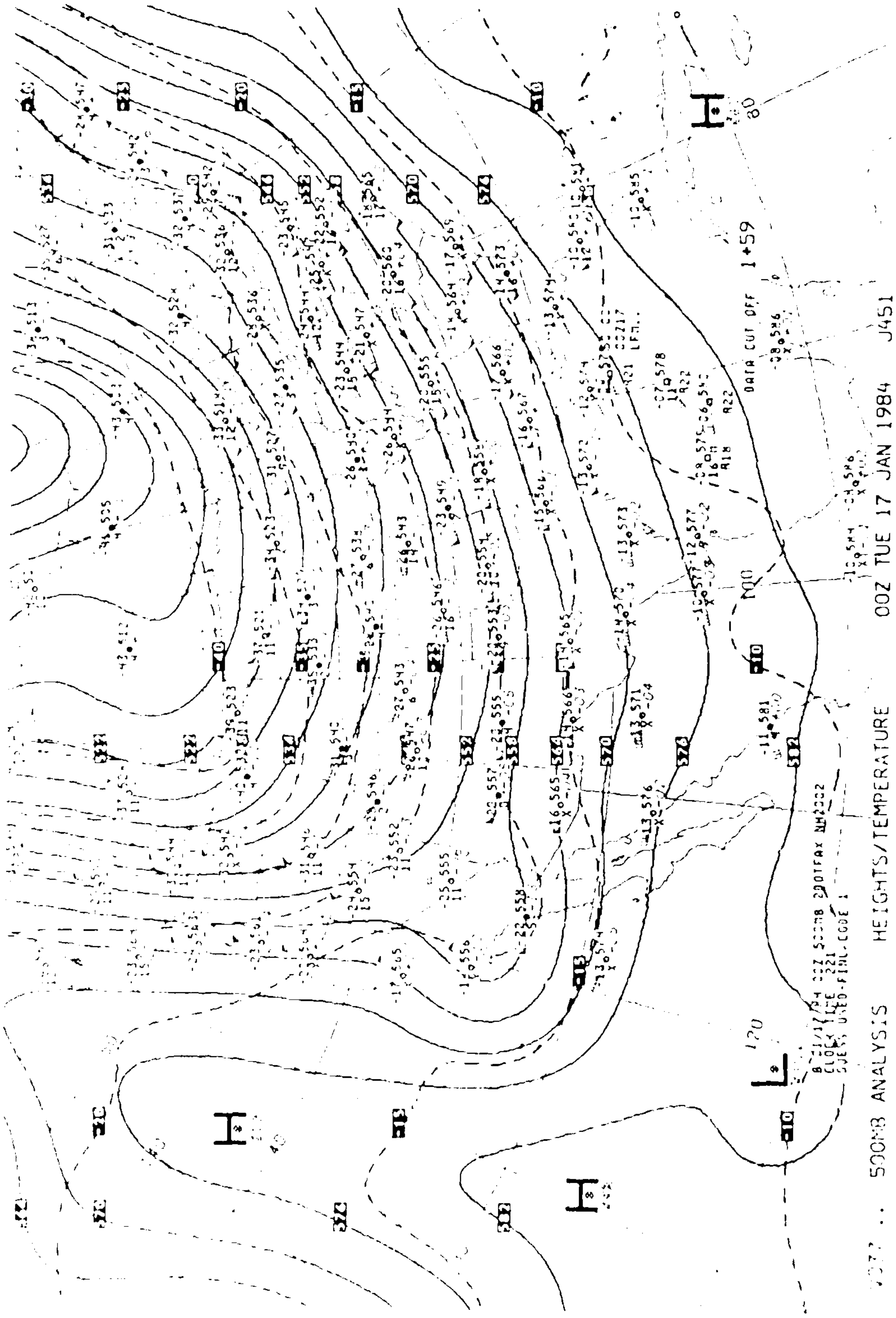

... Constant Pressure Chart at 0000 GMT on 17 January 1984.

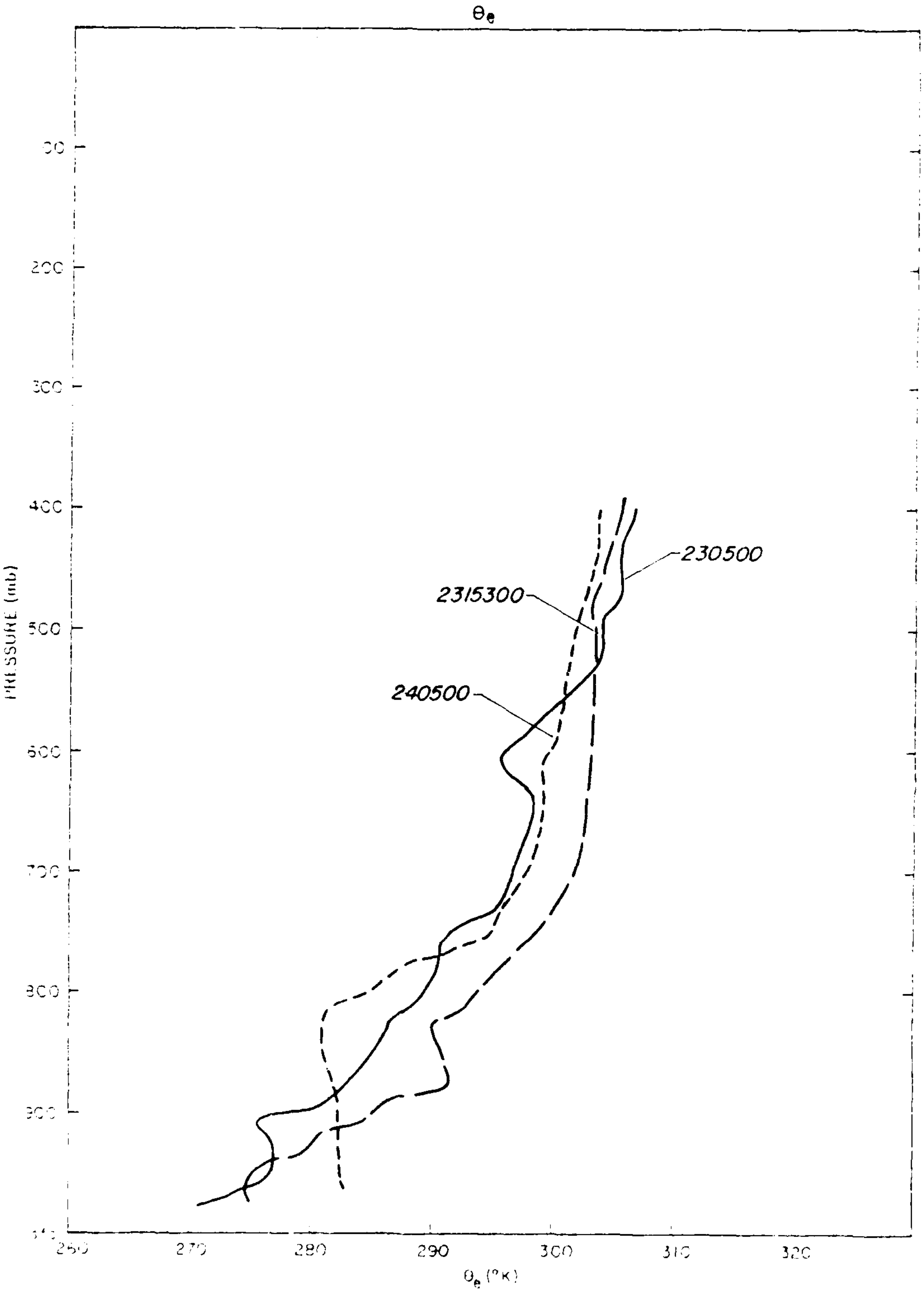

Figure 31. Vertical Profiles of Equivalent Potential Temperature at Camp Grayling, MI at 0500 GMT 23 January, (230500), 1530 GMT 23 January (231530), and 0500 GMT 24 January (240500) 1984.

4.4 Time Series of Rawinsonde Observations at Camp Grayling

The cold front passed Camp Grayling at approximately 0300 GMT 17 January. Rawinsonde launches were made at 0500 GMT, 1900 GMT 16 January and 0500 GMT, 1900 GMT 17 January. Figures 50, 51, 52 and 53 show the vertical profiles of zonal wind, meridional wind, potential temperature, and equivalent potential temperature in time series. In contrast to the 23-24 January case, Figure 51 again shows the meridional wind was weak in general. The increase in the zonal wind between 0500 GMT 16 January and 0500 GMT 17 January is very striking (Figure 50). It seems that the increase in the zonal current in the mid-troposphere was at least partially related to the north-south pressure gradient due to the presence of the low pressure center situated over northern Canada (Figure 32) in the mid-troposphere associated with the surface frontal system. The ageostrophic component may have contributed to the strong zonal wind (which reached 69 m sec^{-1} at 200 mb) as suggested by Uccellini and Johnson (1979), especially in the upper troposphere.

Both the potential temperature and the equivalent potential temperature show decreases after the passage of the cold front in the low troposphere (Figures 52 & 53). A well mixed layer near the ground surface was clearly shown for both the 0500 GMT and the 1900 GMT 17 January soundings after the cold front passage. The top of the inversion rose during the passage of the cold front and dropped behind the cold front due to the presence of the surface convergence. The convective clouds may have been able to develop to the top of inversion in the frontal zone and behind the front. Further growth of the convective clouds above the top of the inversion with cloud base rooted in the boundary layer may not have been possible. As discussed before, the cold clouds and precipitation were mainly maintained by the ascending motion of the warm moist air above the frontal surface. Since the upper level jet maximum was located at 200 mb which was above the main divergence outflow layer found between 300 to 400 mb, this would exclude a possibility of the upper level jet playing an important role in initiating convective activities for this case.

There are two possible causes for the well mixed layer capped with the inversion behind the surface cold front:

a. The prevailing subsidence behind the cold front as suggested by Ogura and Portis (1982)

b. The inversion may have represented the interface between the cold arctic continental air near the ground surface and the warm dry air above.

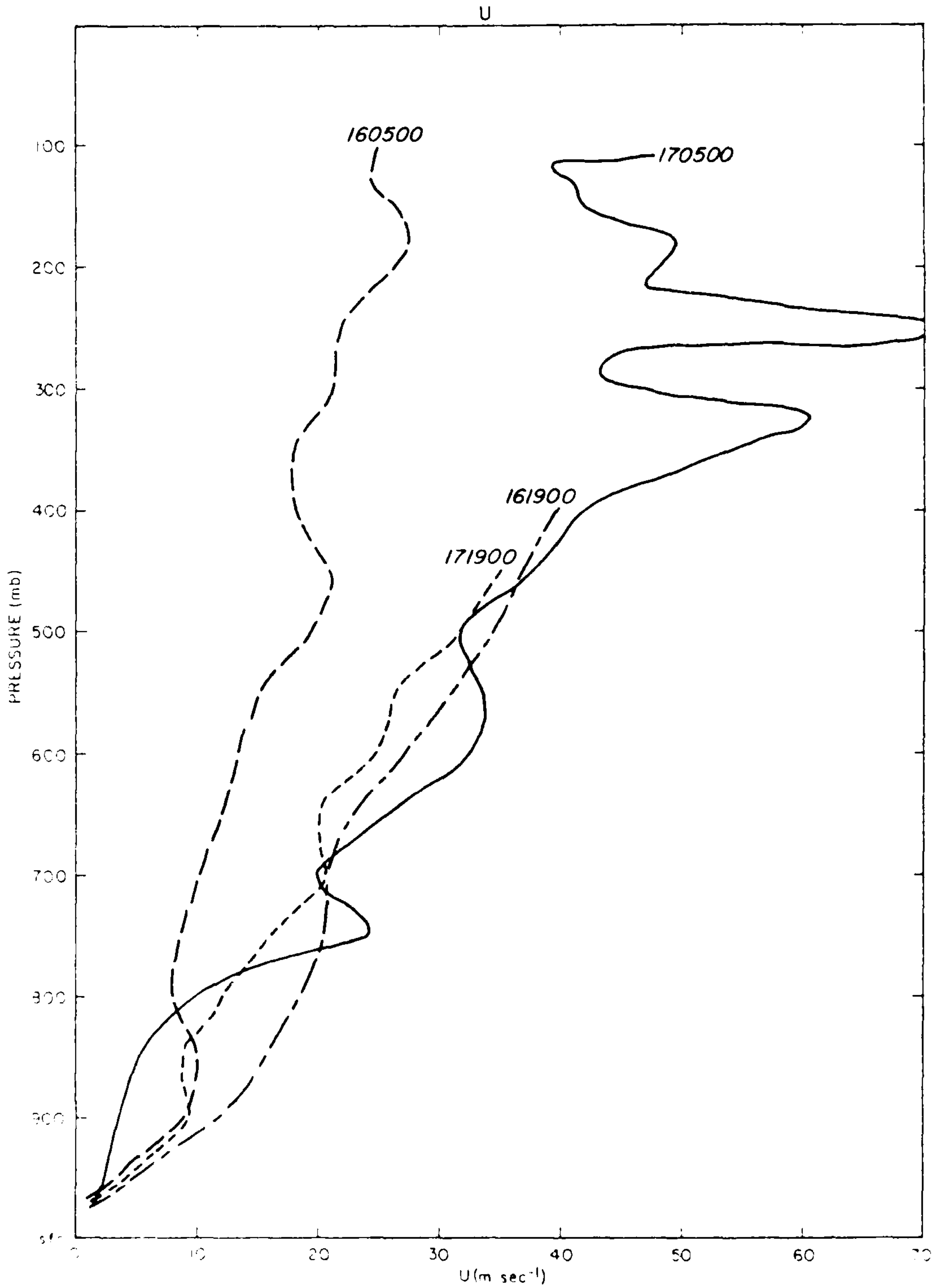

Figure [illegible]. Vertical Profiles of Zonal Wind at Camp Grayling, MI at 0500 GMT 16 January, (160500), 1900 GMT 16 January (161900), 0500 GMT 17 January (170500), and 1900 GMT 17 January (171900) [illegible].

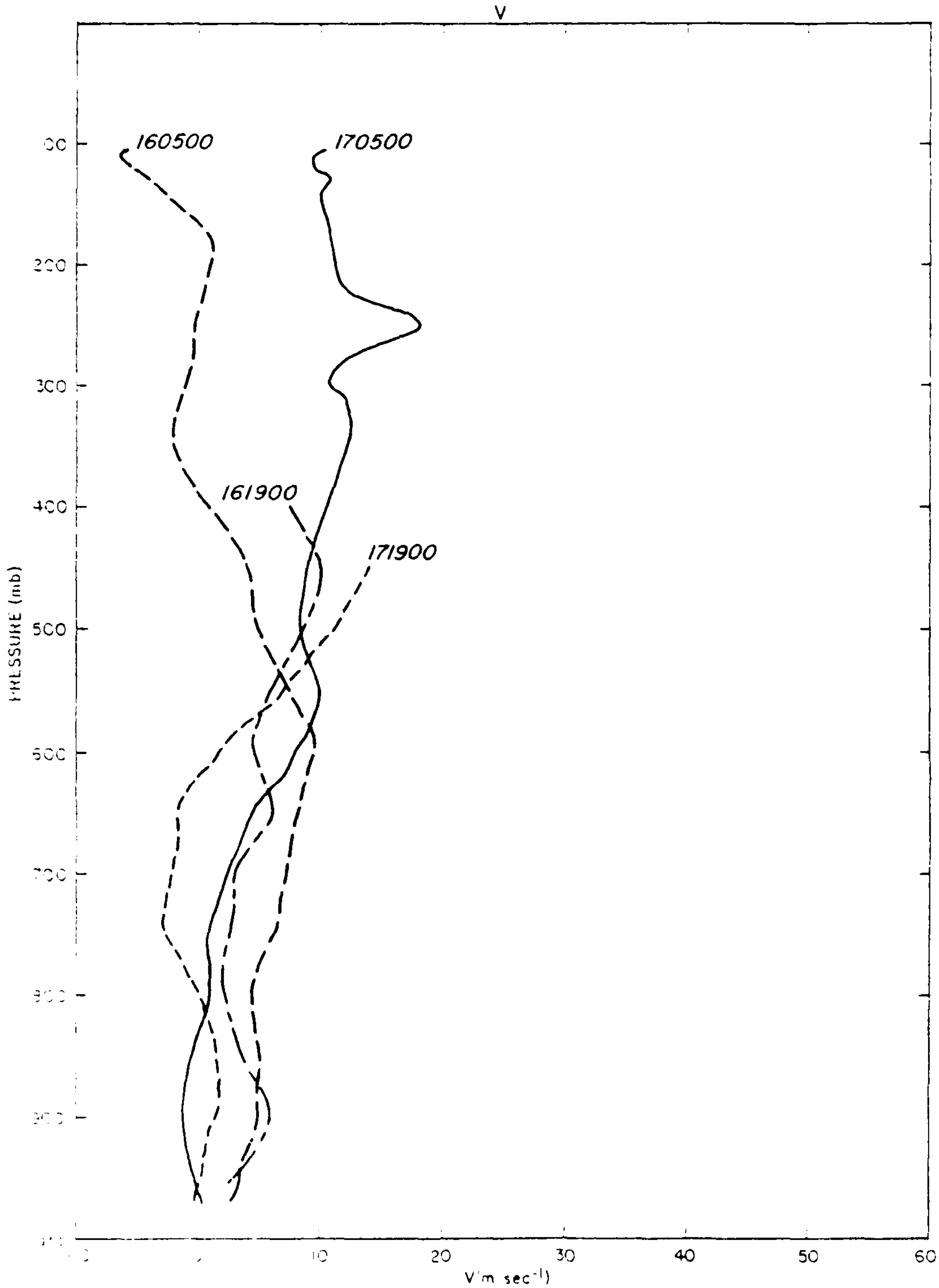

Figure [illegible]. Vertical Profiles of Meridional Wind at Camp Grayling, MI at 0500 GMT 16 January, (160500), 1900 GMT 16 January (161900), 0500 GMT 17 January (170500), and 1900 GMT 17 January (171900), 1984.

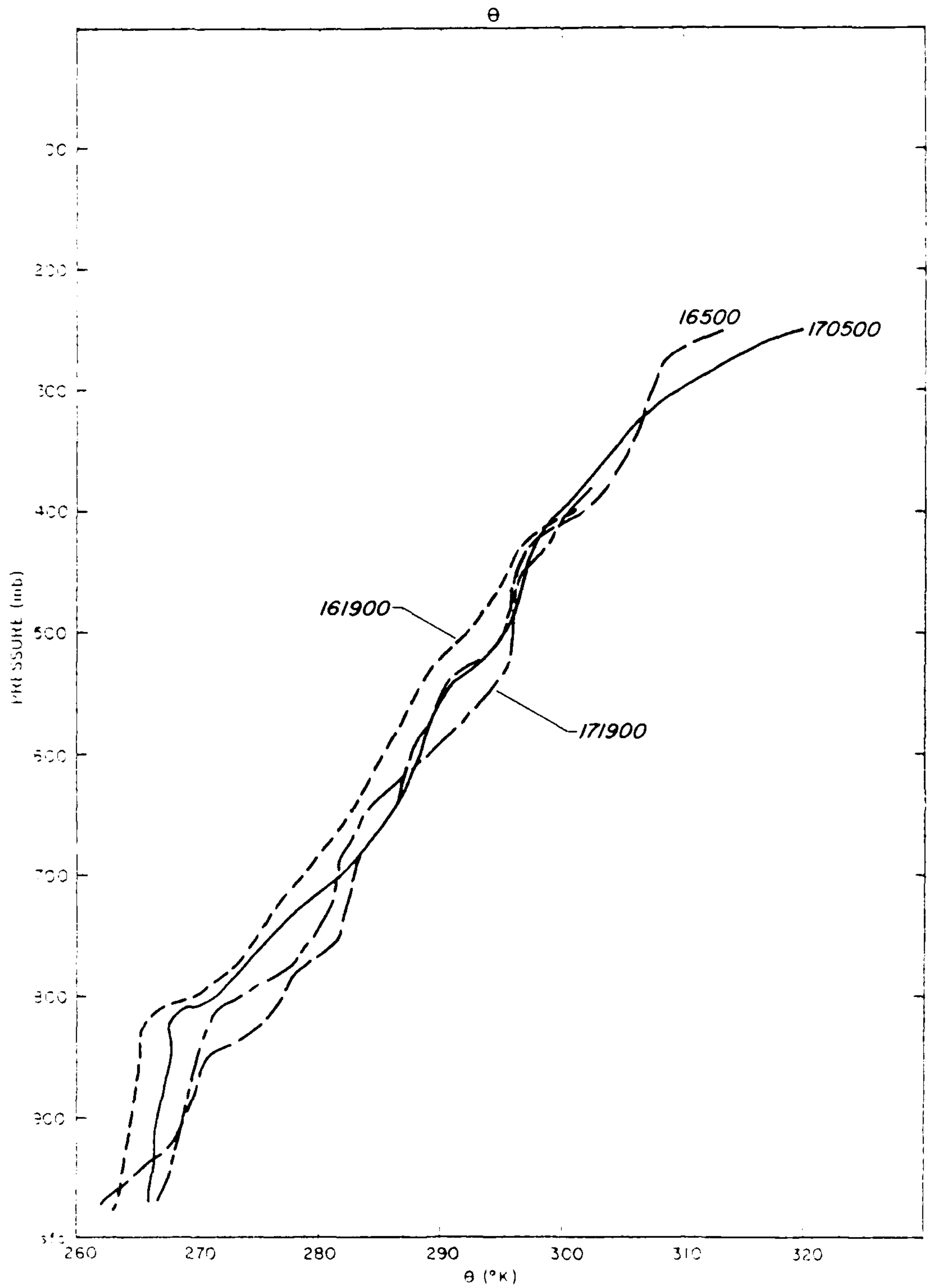

Figure 2. Vertical Profiles of Potential Temperature at Camp Grayling, MI at 0500 GMT 16 January, (160500), 1900 GMT 16 January (161900), 0500 GMT 17 January (170500), and 1900 GMT 17 January (171900) 1984.

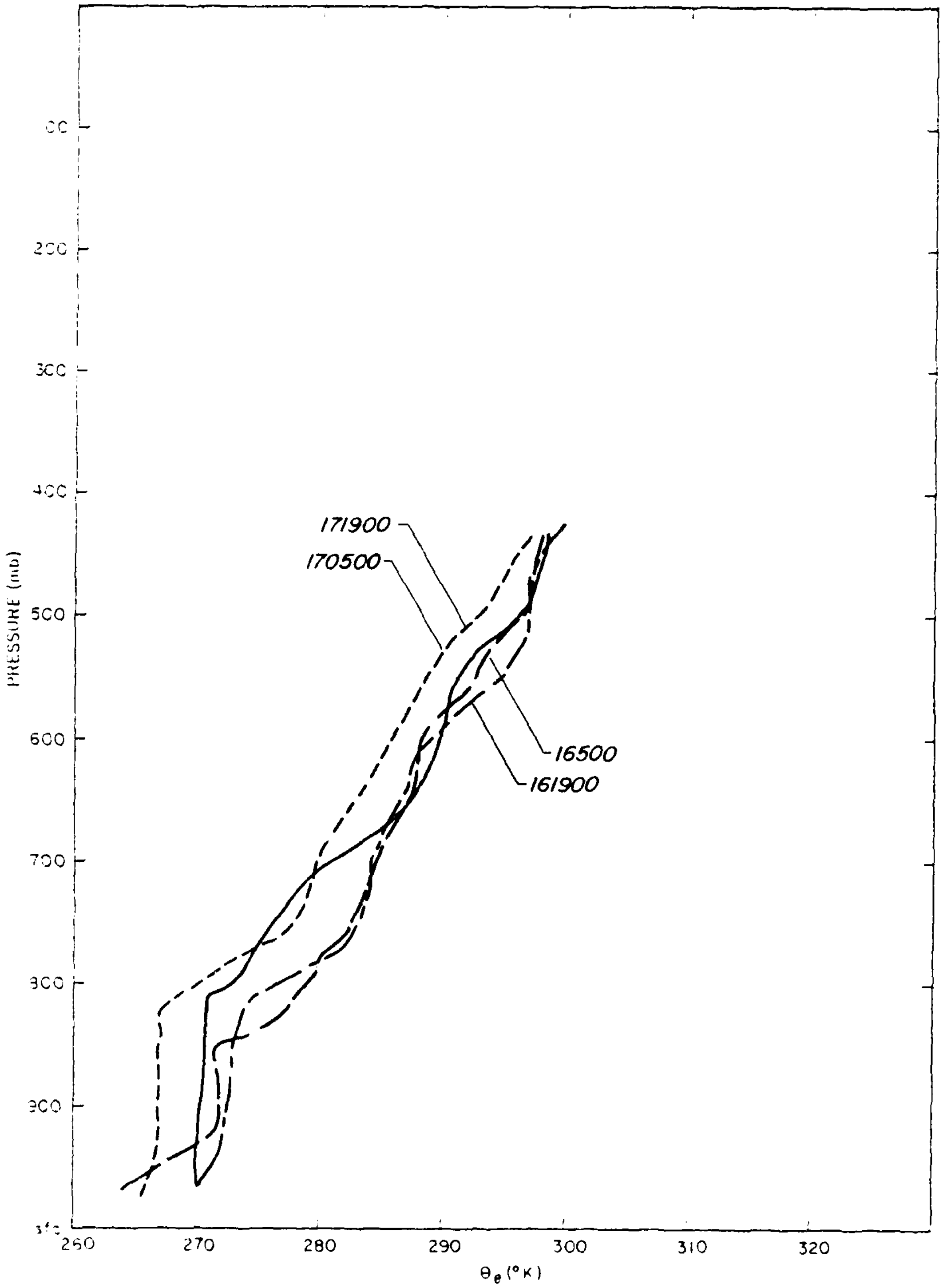

Figure 53. Vertical Profiles of Equivalent Potential Temperature at Camp Grayling, MI at 0500 GMT 16 January, (160500), 1900 GMT 16 January (161900), 0500 GMT 17 January (170500), and 1900 GMT 17 January (171900) 1984.

7. CONCLUSIONS

Two case studies of snowstorms which occurred during SNOW TWO, namely 23-24 January and 16-17 January, were made using NWS regular 12 hr rawinsonde data, hourly surface data, satellite data, and surface observations and upper-air observations taken at Camp Grayling, MI. The physical processes which were responsible for the clouds and precipitation for both cases appeared to be quite different.

The analyses for the 23-24 January case showed that the region of deep convection was along the axis of the southerly wind maximum. A high pressure center was situated over the east coast. The west-east pressure gradient increased as a trough intensified in the west. As a result, the speed of the meridional wind increased. The strong meridional wind brought in the warm and moist air from the south in the middle and low troposphere resulting in a conditionally unstable atmosphere above 700 mb. Finally, the large-scale lifting triggered the deep convection and the release of potential instability

For the 16-17 January case, a cold front passed Camp Grayling, MI. approximately at 0300 GMT 17 January. Sharp horizontal temperature and equivalent potential temperature gradients were found below 850 mb in the frontal zone. It is important to note that the atmosphere was stable both ahead of and behind the surface front except below the temperature inversion near the ground surface. After the passage of the arctic cold front, a well mixed layer was evident below the inversion which separated the cold arctic continental air below and warm air above. Subsidence was found behind the cold front which confined the cold air below the inversion. The ascending motion of warm moist air over and ahead of the surface cold front apparently initiated and sustained the convection. As the cold front and the cold air behind it moved eastward, the relatively warm and moist air was lifted, became saturated and produced precipitation.

6. REFERENCES

Chang, S.W., and H.D. Orville, 1973: Large-scale convergence in a numerical cloud model, J. Atmos. Sci., 30, 947-950.

Cline, A.K., 1973: Curve fitting using splines under tension, Atmos. Tech., No. 3, NCAR, 60-65.

Cotton, W.R., 1975: On parameterization of turbulent transport in cumulus clouds, J. Atmos. Sci., 32, 548-564.

Cotton, W.R., R.A. Pielke, and P.T. Grannon, 1976: Numerical experiments on the influence of the mesoscale circulation on the cumulus scale, J. Atmos. Sci., 33, 252-261.

Cressman, G.P., 1959: An operational objective analysis system, Mon. Wea. Rev., 87, 367-374.

O'Brien, J.J., 1970: Alternative solution to the classical vertical velocity problem, J. Appl. Meteor., 9, 197-203.

Ogura, Y., and Y.-L. Chen, 1977: A life history of an intense mesoscale convective storm in Oklahoma, J. Atmos. Sci., 33, 1458-1476.

Ogura, Y., Y.-L. Chen, J. Russell, and S.-T. Soong, 1979: On the formation of organized convective systems observed over the eastern Atlantic, Mon. Wea. Rev., 107, 426-441.

Ogura, Y., and D. Portis, 1982: Structure of the cold front observed in SESAME-AVE III and its comparison with the Hoskins-Bretherton Frontogensis model, J. Atmos. Sci., 39, 2773-2792.

Panofsky, H.A., 1946: Methods of computing vertical motion in the atmosphere, J. Meteor., 3, 45-49.

Pielke, R.A., 1974: A three-dimensional model of the sea breezes over South Florida, Mon. Wea. Rev., 102, 115-139.

Soong, S.-T., and Y. Ogura, 1980: Response of tradewind cumuli to large-scale processes, J. Atmos. Sci., 37, 2035-2050.

Soong, S.-T., and W.-K. Tao, 1980: Response of deep tropical cumulus clouds to mesoscale processes, J. Atmos. Sci., 37, 2016-2034.

Uccellini, L.W., and D.R. Johnson, 1979: The coupling of upper and lower tropospheric jet streaks and implications for the

development of severe convective storms., Mon. Wea. Rev., 107, 682-703.

Wang, J.Y.C., 1984: A preliminary numerical simulation of a shower, J. Atmos. Sci., 41, 789-806.

APPENDIX I - Upper Boundary Condition for the Vertical Motion

In this study, the upper boundary condition $w=0$ was imposed at 100 mb using O'Brien's (1970) scheme. The vertical cross section of vertical velocity and divergence obtained by imposing the upper boundary condition $W=0$ at 200 mb for 1200 GMT 23 January are shown in Figures 54 and 55 of this Appendix for comparison.

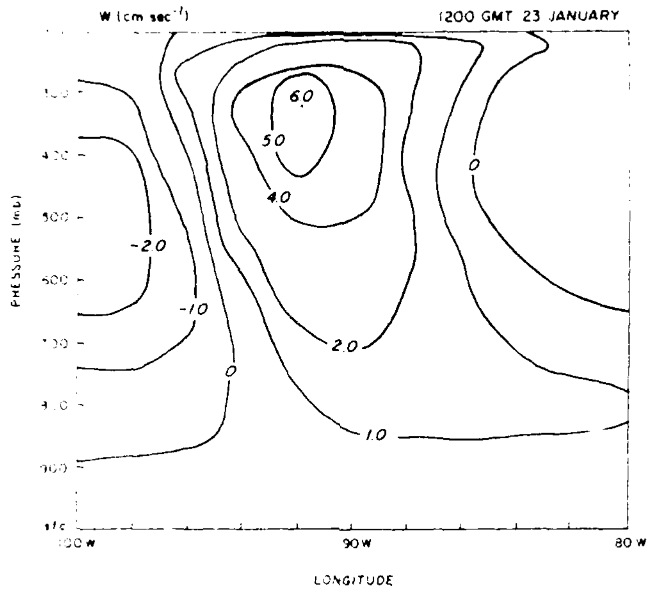

Figure [illegible]4. Vertical, West-East Cross Sections of Vertical Velocity Averaged from 40 degrees N through 42 degrees N for 1200 GMT on 23 January 1984.

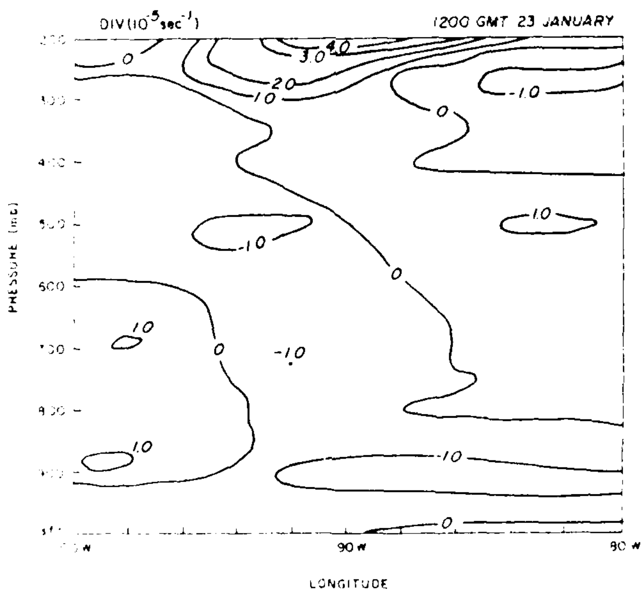

Figure [illegible]. Vertical, West-East Cross Sections of Divergence Averaged from 40 degrees N through 42 degrees N for 1200 GMT on 23 January 1984.

8. APPENDIX 2 - Procedure to Process Upper-Air Data For Snow Two

The outline for the procedures to process upper-air data is given below:

```
DATA TAPE-- R DATA-- VAX DISK-- PROGRAM DECSNG
-- OUTPUT DATA FILE -- PROGRAM SGENT
-- OUTPUT DATA FILE -- TRANSFER DATA TO CDC
   PROGRAM LARR7 -- OUTPUT DATA FILE
-- PROGRAM HORSPL7 -- OUTPUT DATA FILE
-- WW -- OUTPUT DATA FILE -- WMPRT (OR CROSS) -- OUTPUT LISTINGS
```

Both Program DECSNG and SGENT are on the VAX. The output file from SGENT which contains soundings with 25 mb intervals is transferred to the CDC file directory. This data file is rearranged into 37 records (Program LARR7). Each record contains data from all stations for the same pressure level from the surface to 100 mb. Finally the analysis routine HORSPL7 is used to obtain horizontal distributions of the meteorological variables. The output file from Program DECSNG is also used as an input file for Program THETAE which calculates relative humidity, potential temperature, equivalent potential temperature, and lifting condensation level.

> Note: The output file name for each run on the VAX is FOR0xx.dat. xx is the unit number for the write statement. To use this output file as the input file for another program use the command
>
> RENAME FOR0xx.dat FOR0yy.dat
>
> where yy is the unit number for the read statement in the second program.

Details of the procedures and Job Control Languages to run these programs are described as follows:

Each RAOB form McIDAS has a header record. To run program RDATA.FOR to copy RAOB data to VAX computer, it is necessary to initialize the file number to be copied (NFILE) in the program. The command procedures to mount the tape and run Rdata are:

```
ALLOCATE MTA2(or 3):
MOUNT MTA2(or 3): RAOB FOR001/FOREIGN/
RECORDSIZE=3360/BLOCKSIZE=3360
FORT RDATA
LINK RDATA


RUN RDATA
TYPE FOR002.DAT(To examine the files and records skipped and
number of records read for the file wanted)
DELETE FOR001.DAT
```

```
DEALLOCATE MTA2(or 3):
DISMOUNT MTA2(or 3):
```

The output file contains information for eight periods with 12 hr interval. To run DECSNG to decode the data, it is necessary to specify the data period wanted and the domain considered (see the comment statements in the program). To run the program, use the command procedures:

```
RENAME FOR001.DAT FOR003.DAT
FORT DECSNG
LINK DECSNG,SPLIT
RUN DECSNG
```

There are two output files FOR007.DAT and FOR008.DAT. FOR007.DAT is the input data file for the next program SGFNT. FOR008.DAT contains information for data cycles and time and can be deleted after a listing of FOR008.DAT is obtained. The procedures to run SGFNT are:

```
RENAME FOR007.DAT FOR015.DAT
FORT SGFNT
LINK SGFNT
RUN SGFNT
```

The output files are FOR016.DAT and FOR017.DAT. FOR017.DAT contains information for soundings with 25 mb intervals. This file is transferred to the CDC by typing in the command MUXX (details see Appendix 4). This file is the input data file for UARR7 on the CDC. FOR016.DAT has information for both input data (i.e., mandatory level and significant level data) and output data for each sounding. This file should be examined to check for bad data points. Running SGFNT, one may encounter an overflow problem due to bad data points. When an overflow problem does occur, it is necessary to check and edit the data manually (or add edit statements to the program) to take care of various situations. The resulting 25 mb data should be checked with the original input data carefully. A listing for FOR016.DAT can be obtained by typing in the command PRINT FOR016.DAT. This file can be deleted after SGFNT is run successfully.

The input data for UARR7 on the CDC is the 25 mb soundings calculated by program SGFNT on the VAX. The local file names for input data and output are F1 and F2, respectively. After running this program, the input local file F1 needs to be rewound (or simply return this file). This program can be run interactively using the following commands:

```
ATTACH,UARR7,ID=NEI[illegible]ONED.
ATTACH,F1,DATA1,ID=NEI[illegible]ONED.
[illegible]ARR7.
[illegible]
[illegible]
[illegible]
```

```
REQUEST,A,*PF.
COPY,F2,A.
CATALOG,A,DATA2,ID=NELSONLD.
```

The permanent file DATA2 is the input file for the program HORSPL7. To run HORSPL7 submit a batch job with the JCL as follows:

```
[illegible](T=100,CM=77000)
ATTACH,A,HORSPL7,ID=NELSONLD.
FTN,I=A,SL,R=3,FL=12000.
ATTACH,B,DATA2,ID=NELSONLD.
LGO,B)
REWIND,F2.
REQUEST,C,*PF.
COPY,F2,C.
CATALOG,C,OLDDATA,ID=NELSONLD.
[illegible]
.
```

The permanent file OLDDATA contains information for horizontal distributions of vertical motion, divergence, vorticity, zonal wind, meridional wind, temperature, dew point temperature, and geopotential height. Program WM converts the vertical p-velocity to cm sec^{-1} using the hydrostatic relationship. To run program WM using the following commands

```
ATTACH,A,OLDDATA,ID=NELSONLD.
ATTACH,B,WM,ID=NELSONLD.
FTN,I=B,SL,R=3.
LGO,A)
REWIND,FILE2.
REQUEST,C,*PF.
COPY,FILE2,C.
CATALOG,C,WMDATA,ID=NELSONLD.
```

The permanent data file WMDATA is the final output data file we would like to keep. To obtain an output listing for horizontal distributions (or vertical cross sections) of meteorological fields use the following procedures:

```
ATTACH,A,WMPRT (OR CROSS),ID=NELSONLD.
ATTACH,B,WMDATA,ID=NELSONLD.
FTN,I=A,SL,R=3.
LGO,B)
DISPOSE,OUTFILE,9).
```

The output file FOR017.DAT from program SGENT is also used as input data for CROSS.FOR on the VAX to construct East-West cross sections of meteorological variables form stations 72518, 72528, 72637, 72645, 72655, 72654, near 45 degrees N. The output file FOR021.DAT is the input data for CPL01.FOR to obtain graphic output. Another output file FOR0[illegible].DAT can be deleted after an output listing is obtained.

A program to calculate relative humidity, potential temperature, [illegible] potential temperature, LCL and lifting condensation level [illegible] temperature, dew point and pressure at Camp Grayling is written on [illegible] (SOUNDING.FOR). The input data for each sounding needs to be typed [illegible] manually. A short program to convert wind speed and wind direction [illegible] is also available (WIND.FOR). The output [illegible] be plotted using the IDL graphics facility on the VAX. To invoke [illegible] program PLT.PRO use the following procedures:

[illegible]

[illegible]

[illegible] further details about these programs and the [illegible] can be found in the comment statements within these programs.

9. APPENDIX 3 - Procedures to Process Surface Hourly Data for SNOW TWO

DATA TAPE -- CDC DISK -- PROGRAM SVBC
-- OUTPUT FILE -- PROGRAM HORSPLS

The JCL to copy a file on tape to CDC disk is stored on file JOB1A which is given as follows:

```
jobcard
VSN,TAPE1=SVCA/NT.
REQUEST,TAPE1,NT,HD,L,NS,NORING.
SKIPF(TAPE1,N,17,B)
COPYBF,TAPE1,SVCHEN.
REWIND,SVCHEN.
REQUEST,A,*PF.
COPYBF,SVCHEN, A.
REWIND,A.
CATALOG,A,SVDATA,ID=NELSONLD.
EOR
EOF
```

Note: SVCA is the volume name and N is the number of files to be skipped.

The JCL to run Program SVBC which decodes the desired information is given below.

```
jobcard
ATTACH,A,SVBC,ID=NELSONLD.
FTN5,I=A
ATTACH,B,SVDATA,ID=NELSONLD.
ATTACH,C,DATASV,ID=NELSONLD.
LGO(B,C)
REWIND,TAPE5.
REQUEST,D,*PF.
COPY,TAPE5,D.
CATALOG,D,FILENAME,ID=NELSON.
EOR
EOF
```

Note: It is necessary to specify the time period and the area to be considered on the data file DATASV before running the Program SVBC.

10. APPENDIX 4 - Transferring files between the VAX and CDC

There is a capability on the VAX at AFGL to transfer a file from the CDC to the VAX or from the VAX to the CDC. A command procedure was added to the login command file on username LEE

MCXX:==@DBAO:[USERLIB]MCXX.COM

By typing the command MCXX, we will be able to transfer a file from one computer to another if the file contains only ASCII characters and each record is less than eighty characters. This utility has a built-in help manual. For the account name, we have to enter one of the valid CDC directory names instead of the login password. The password to be entered is the problem number (the number in columns a 50-54 of the jobcard). Other than that, the procedures to transfer a file are described clearly in the help manual.

11. APPENDIX 5 - Horizontal Distributions of Vertical Motion and Divergence

(a) Case of 23-24 January

Horizontal distributions of vertical motion at 700 mb, 500 mb and 300 mb for 1200 GMT 23 January are given in Figures 56, 57, and 58. Horizontal distributions of divergence at surface, 700 mb, 500 mb and 300 mb for 1200 GMT 23 January are given in Figures 59, 60, 61, and 62.

(b) Case of 16-17 January

Horizontal distributions of vertical motion at 700 mb, 500 mb and 300 mb for 0000 GMT 17 January are given in Figures 63, 64, and 65. Horizontal distributions of divergence at surface, 700 mb, 500 mb and 300 mb for 0000 GMT 17 January are given in Figures 66, 67, 68 and 69.

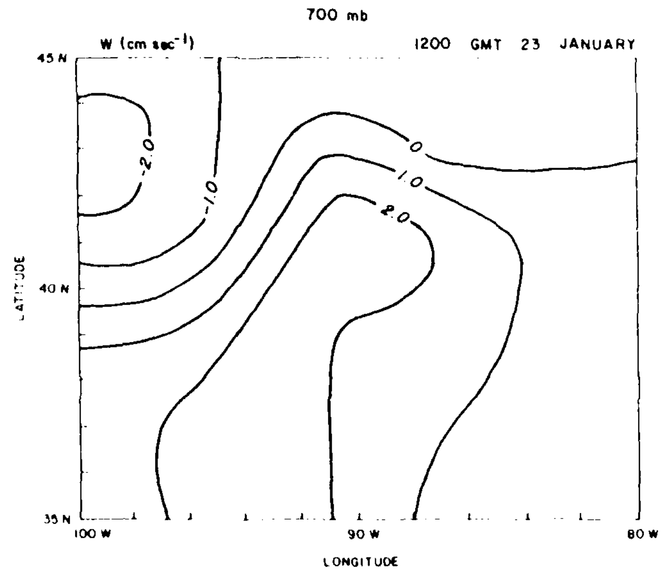

Figure 56. Horizontal Distribution of Vertical Velocity at 700 mb for 1200 GMT on 23 January 1984.

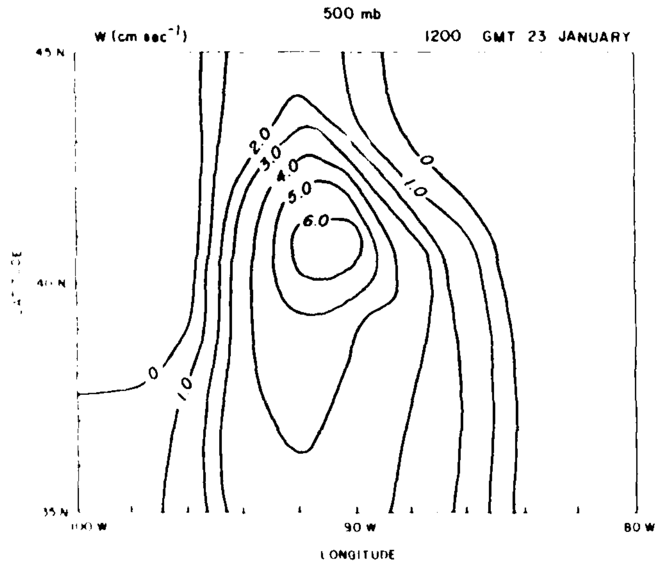

Figure 57. Horizontal Distribution of Vertical Velocity at 500 mb for 1200 GMT on 23 January 1984.

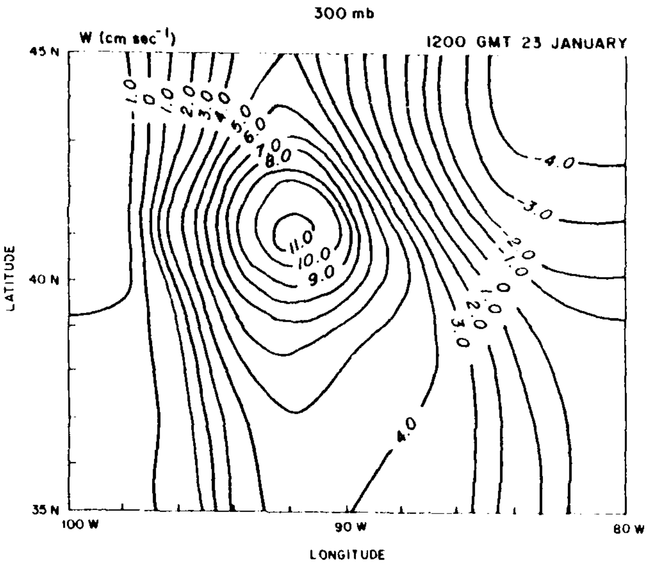

Figure 58. Horizontal Distribution of Vertical Velocity at 300 mb for 1200 GMT on 23 January 1984.

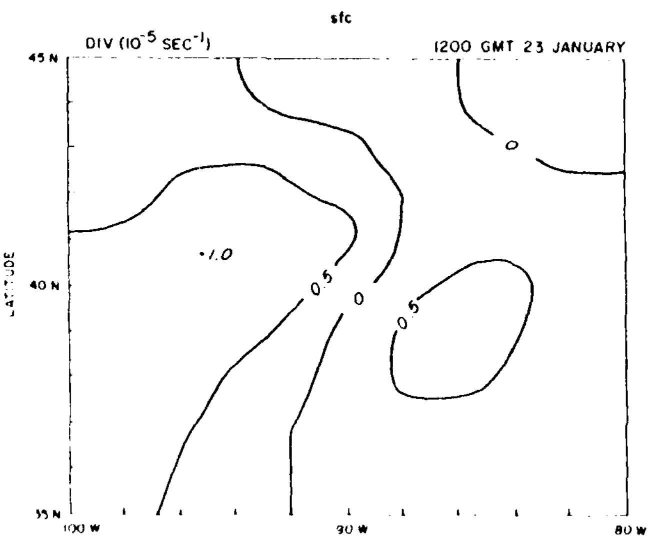

Figure 59. Horizontal Distribution of Divergence at the Surface for 1200 GMT on 23 January 1984.

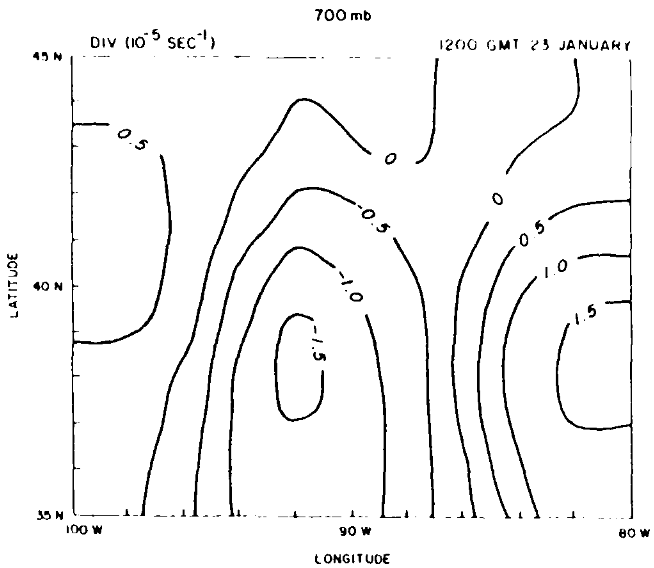

Figure 60. Horizontal Distribution of Divergence at the 700 mb for 1200 GMT on 23 January 1984.

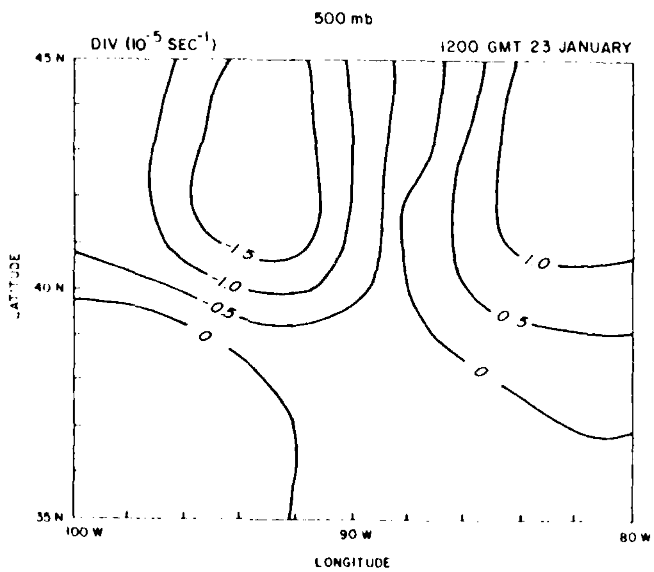

Figure 61. Horizontal Distribution of Divergence at the 500 mb for 1200 GMT on 23 January 1984.

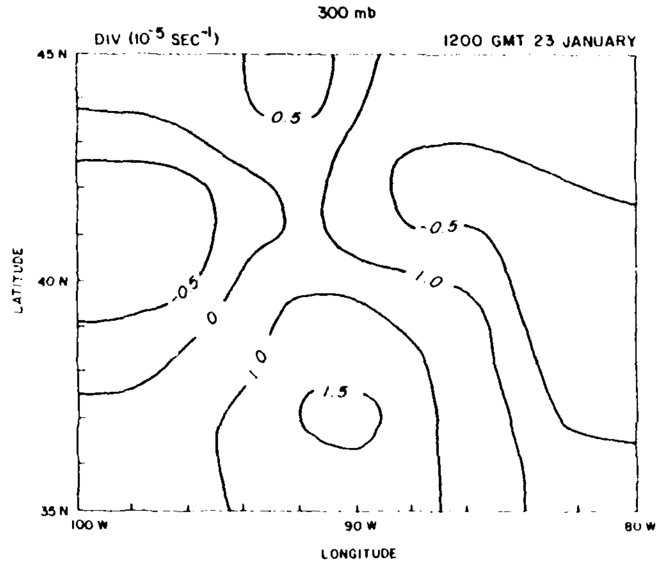

Figure 62. Horizontal Distribution of Divergence at the 300 mb for 1200 GMT on 23 January 1984.

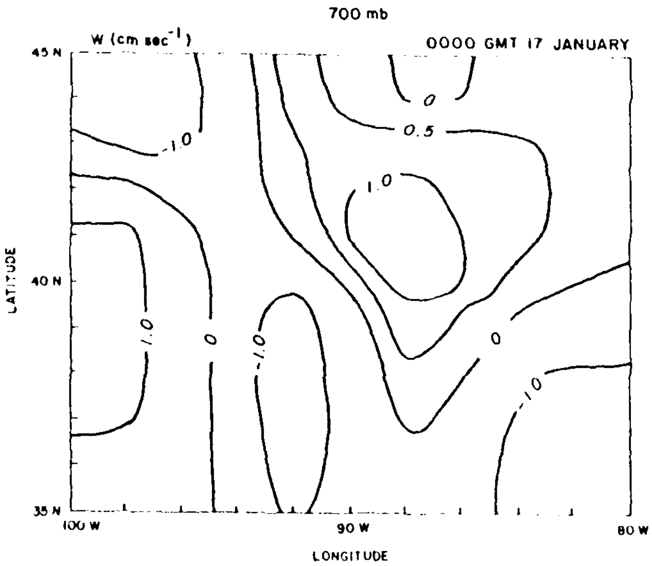

Figure 63. Horizontal Distribution of Vertical Velocity at 700 mb for 0000 GMT on 17 January 1984.

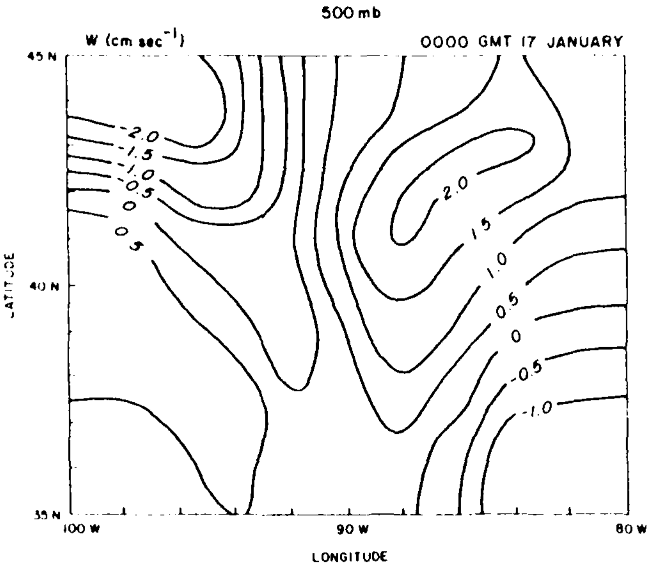

Figure 64. Horizontal Distribution of Vertical Velocity at 500 mb for 0000 GMT on 17 January 1984.

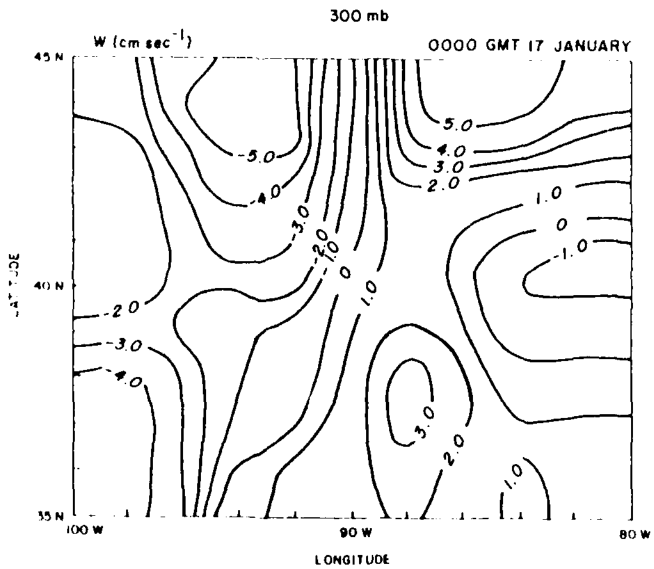

Figure 65. Horizontal Distribution of Vertical Velocity at 300 mb for 0000 GMT on 17 January 1984.

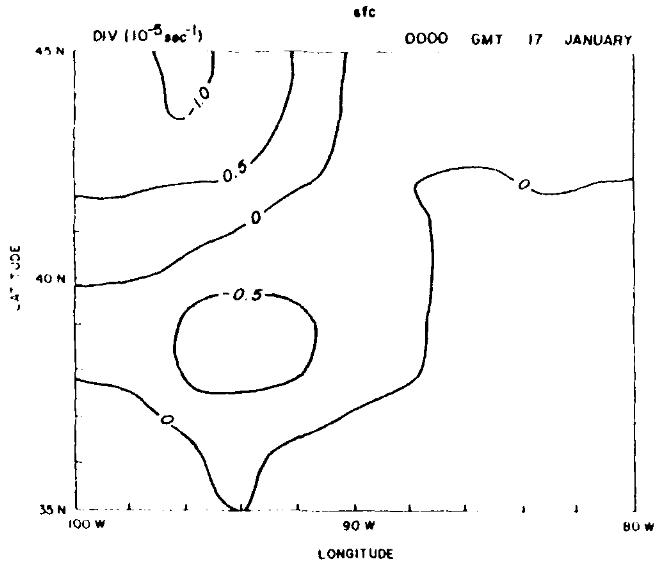

Figure 66. Horizontal Distribution of Divergence at the Surface for 0000 GMT on 17 January 1984.

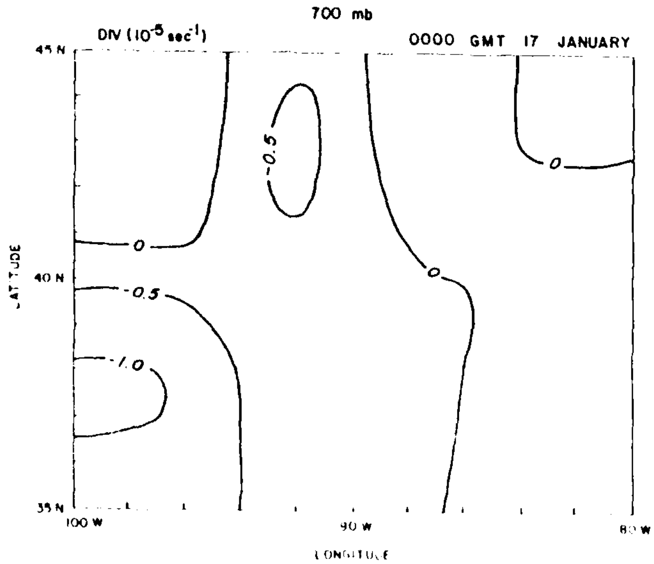

Figure 67. Horizontal Distribution of Divergence at the 700 mb for 0000 GMT on 17 January 1984.

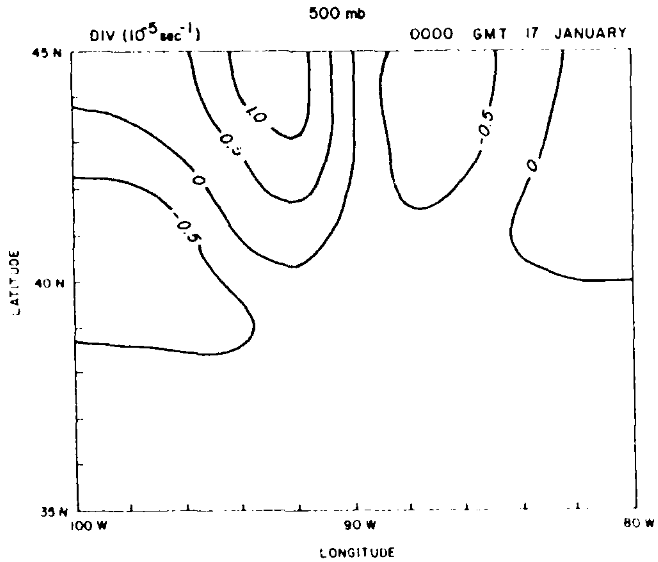

Figure 68. Horizontal Distribution of Divergence at the 500 mb for 0000 GMT on 17 January 1984.

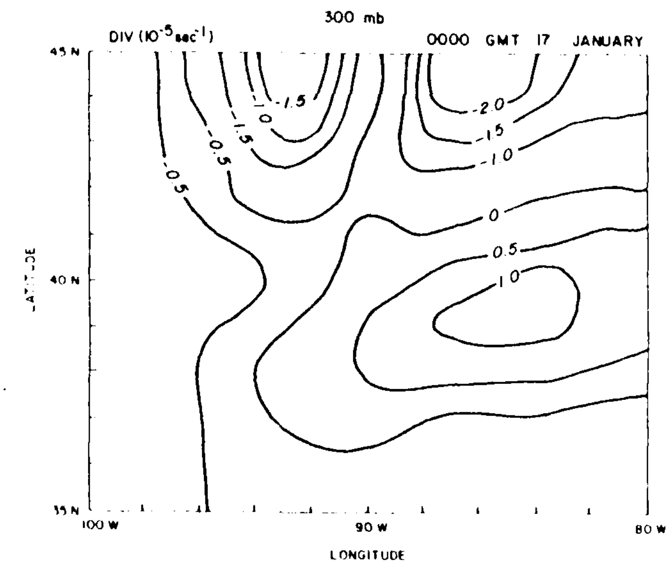

Figure 69. Horizontal Distribution of Divergence at the 300 mb for 0000 GMT on 17 January 1984.

12. APPENDIX 6 - Supplementary Analyses

Analyses for 0000 GMT 24 January and 1200 GMT 17 January were made. The analyses for these time periods are less consistent with the observed convective activities. For completeness, the vertical cross sections of vertical motion and divergence for 0000 GMT 24 January and 1200 GMT 17 January are shown in Figures 70, 71, 72, and 73, respectively.

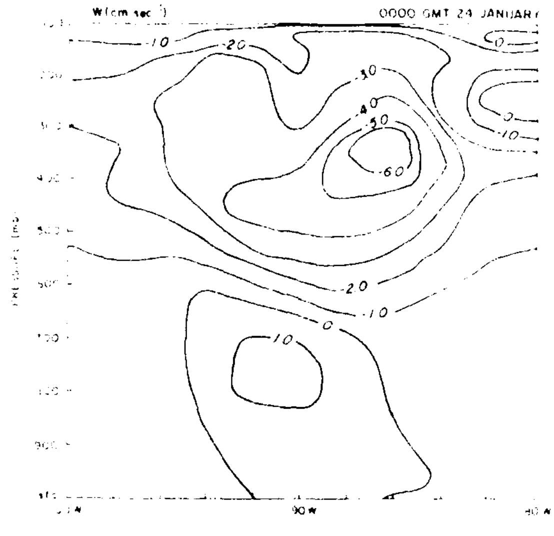

Figure 70. Vertical, West-East Cross Sections of Vertical Velocity Averaged from 40 degrees N through 42 degrees N for 0000 GMT on 24 January 1984.

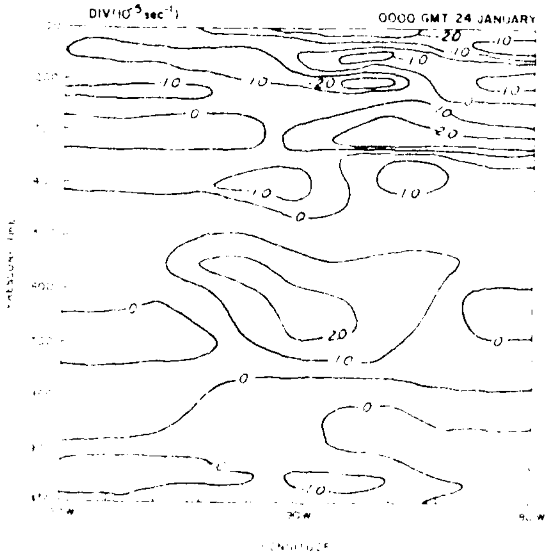

Figure 71. Vertical, West-East Cross Sections of Divergence Averaged from 40 degrees N through 42 degrees N for 0000 GMT on 24 January 1984.

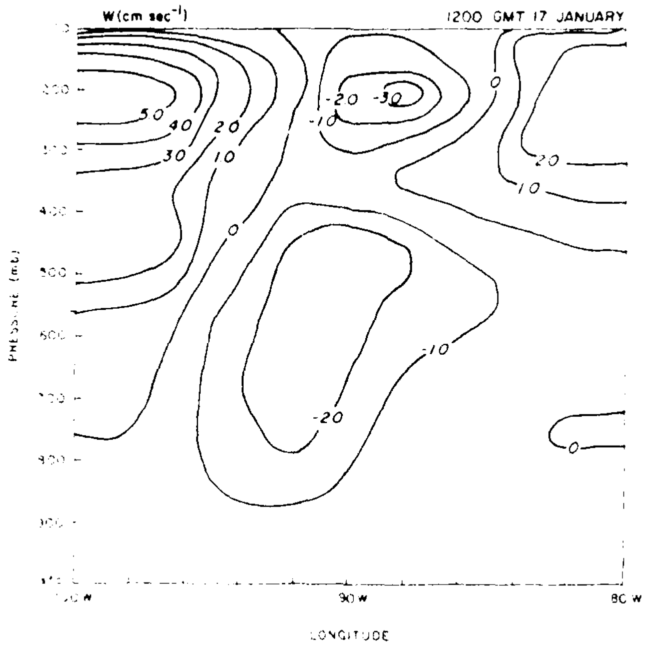

Figure [illegible]. Vertical, West-East Cross Sections of Vertical Velocity Averaged from 40 degrees N through 42 degrees N for 1200 GMT on 17 January 1984.

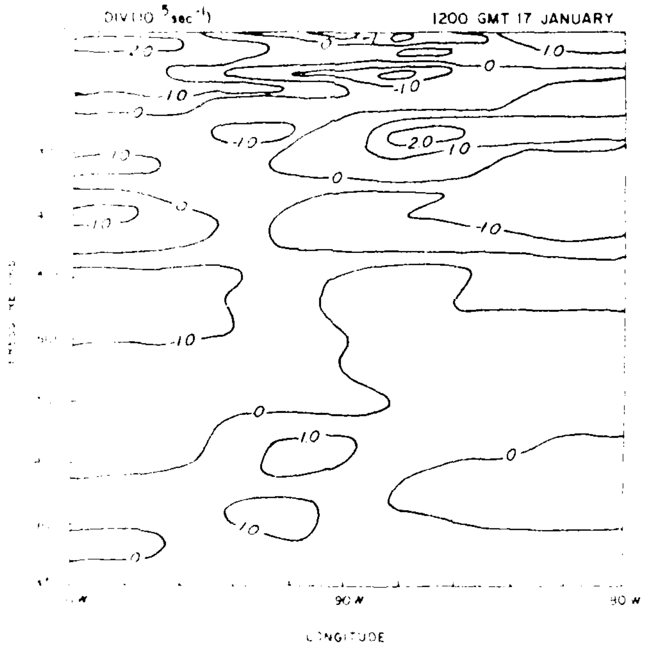

Figure [illegible]. Vertical, West-East Cross Sections of Divergence Averaged from 40 degrees N through 42 degrees N for 1200 GMT on 17 January 1984.

END

FILMED

7-85

DTIC